International Journal of Dynamics and Control (2019) 7:1462–1488
https://doi.org/10.1007/s40435-019-00517-w

Biomechanics, actuation, and multi-level control strategies of power-augmentation lower extremity exoskeletons: an overview

Hayder F. N. Al-Shuka[1] · Mohammad H. Rahman[2] · Steffen Leonhardt[3] · Ileana Ciobanu[4] · Mihai Berteanu[4,5]

Received: 7 January 2019 / Revised: 27 January 2019 / Accepted: 29 January 2019 / Published online: 6 February 2019

Abstract
Improper manipulation of heavy objects can result in hard stresses (tension, compression and shear) throughout the human body parts, especially in the low-back spine. Biomechanics specialists state that injuries that occur in this area may address muscle tissue, joint tissues and intervertebral disc tissues. The effect of a carried load on kinematics and kinetics of body's lower extremity is significant. Besides of labor protection rules and interventions designed to reduce and avoid injuries, powered wearable exoskeletons have been proposed to amplify human capabilities. The paper regards three significant issues related to exoskeletons: biomechanical modeling, actuation, and multi-level control strategies. Three modalities to get optimal performance of wearable robots are hereby summarized: (i) minimization of interaction force wrench by using direct/indirect force control strategies, (ii) modification of reference trajectory to compensate for unwanted interaction force wrench, and (iii) adding the power assist rate such that zero impedance at interaction attachments is guaranteed. To accomplish these points, most proposed control strategies consist of three levels of control: high-level control, responsible for capturing human movement intention; mid-level control for regulation of divisions of the gait cycle; and low-level control for stabilization of the coupled motion.

Keywords Human walking intention · Lower extremity exoskeleton · Biomechanics · Impedance control · Biped locomotion

1 Introduction

Exoskeleton is a term borrowed from biology, where it refers to the chitin hardcover of the insects, used for support and protect purposes [1]. Inspired by the biology field, human exoskeleton suits are wearable robots that can be powered by electromechanical, hydraulic, pneumatic actuators, etc. for enhancing the user's (wearer's/operator's/pilot's) strength, endurance and speed [1]. In general, exoskeletons can be classified as upper extremity exoskeleton, lower extremity exoskeleton, full exoskeleton suit, or smaller body part exoskeleton, e.g., hand exoskeleton, hip joint exoskeleton, etc. However, this work is focused on lower extremity exoskeletons (LEEs) with power amplification for non-disabled users' physical activities assistance.

Biomechanics studies show severe injuries that can be produced by carrying heavy loads; the possible injured parts are back, knee, ankle, or shoulder, etc. In addition, the torques generated at hip, knee, and ankle level increase proportionally to the carried loads. In view of the above, a load carrying exoskeleton is expected to reduce the risk and severity of an injury as well as the energy expenditure of the user [2–5]. The idea behind the design of powered exoskeletons (PEs) is to combine human intelligence and robot strength to perform some dangerous and difficult civil and military tasks such as rescue work, firefighting, war field missions, but assistance and rehabilitation of people with locomotor disabilities, as well [6, 7]. Walking assistance requires harmony

✉ Hayder F. N. Al-Shuka
hayder.al-shuka@rwth-aachen.de

1 School of Control Science and Engineering, Shandong University, Jinan, China

2 Mechanical/Biomedical Engineering Department, University of Wisconsin-Milwaukee, Milwaukee, USA

3 The Philips Chair for Medical Information Technology (MedIT), Helmholtz-Institute for Biomedical Engineering, RWTH Aachen University, Aachen, Germany

4 Rehabilitation Medicine Department, Elias University Hospital, Bucharest, Romania

5 Rehabilitation Medicine Department, Carol Davila University of Medicine, Bucharest, Romania

between the user's intentions and exoskeleton's action. The exoskeleton provides force assistance and support to the user while he/she can adapt his/her muscle activation patterns, lower muscle forces and energy consumption being required from the user [8]. The exoskeleton and the user are in contact at a variety of places, such as feet, shanks, thighs, etc. imposing interaction forces wrench (forces and torques) between the exoskeleton and the user [6]. The need to integrate human and exoskeleton together and making them as one whole system complicate the prerequisite control algorithms, due to the coupled dynamics and kinetic–kinematic restrictions. Design and control of rehabilitation devices for movement force and trajectory training is easier than human–machine integration for power augmentation, due to limited number and complexity of the activities the system must perform [9].

The earliest exoskeleton device developed by Yagn in 1890 was a passive system acting in parallel to the user's lower limbs with longbow springs for facilitating human walking, running and jumping [10]. In 1917, Kelly designed a steam-powered device for supporting human walking and running. A small steam engine carried on the back by the user, actioned on artificial ligaments designed in parallel to the major muscle ligaments of the user [11]. Then exoskeleton field witnessed a long period of languishment for some decades. In early 1960s, a team from Cornell aeronautical laboratory, supported by the U.S. Defense Department, developed a full human body exoskeleton with fewer degrees of freedom for the user and actuated with hydraulic actuators, designed for enhancing user's power. Master–slave control was proposed as a basis for tracking the user motion and regulating the interaction forces [12, 13]. The aim of the project was to imitate the full motion of the human user. At the same time, the US General Electric developed Handiman exoskeleton [6, 14–16]. It consists of two overlapping exoskeletons with 30 degrees of freedom (DoFs) powered by hydraulic actuators. While it was designed to lift 680 kg, the exoskeleton was too heavy and had limitations regarding joint dexterity and hydraulic control technology [17]. Reproducing all human movements and using master–slave robotic systems can have some practical limitations [6]. In 1969, Vukabratovic and his colleagues at the University of Belgrade developed some powered exoskeletons for aiding people with paraplegia [18–20]. Despite the limitations of Belgrade devices, stabilization and balancing criterion, which is the so-called zero-moment point (ZMP) are still used in most biped robots [21–30]. In the mid-1980s, Pitman suit was conceived by Los Alamos National Laboratory. It was a full powered suit of armor for infantrymen controlled by a network of brain-scanning sensors in the helmet [17]. These attempts were not successful due to some problems associated with technology limitations. The major limitations of exoskeleton design can include the power supply, actuators and joint flexibility, power control and modulation, and adaptation to the user size variations. From early 1990s onwards, practical powered exoskeletons have been developed for power augmentation. Some examples of these models are HAL suit of Tsukuba University [31–38], RoboKnee of MIT [7], and BLEEX of California University [6, 39–41], etc. the details will be described later throughout this paper.

In summary, there are important points that should be considered for designing the Pes [7, 8, 42]:

- The exoskeleton should be comfortable with a natural interface.
- The exoskeleton should follow the user intention and apply forces when and where suitable, with low impedance to the user. The user's muscles should exert lower forces than when the user performs the same task without exoskeleton assistance.
- The joint angle trajectory of the coupled user-exoskeleton system should be modifiable while walking.
- Attention should be paid to the human biomechanics during walking, e.g., how to support the weight and propel the human body in a naturally functional manner
- Motion synchronization of the coupled user-exoskeleton system.
- The interaction forces/torques between the user and the exoskeleton should carefully be considered and minimized.
- The user plays important role in the control of the worn exoskeleton.
- Human motion in irregular terrains may make the control problems more complex.
- Three important issues should be considered for control purposes: estimation (detection/measurement) of the human–exoskeleton interaction forces/torques, estimation of the intended human motion, and the feasible control strategy.

Despite several previous reviews have considered design and control issues of LEEs [43–49], they did not present a unified control architecture for the target LEEs. The current work is focused on resolving this problem introducing a systematic review on challenging issues of the LEEs.

This paper is organized as follows: Sect. 2 introduces biomechanics of the human lower extremity. Actuation of the exoskeleton is presented in Sect. 3. Section 4 includes dynamics of the LEEs. Section 5 investigates the major control strategies for the LEEs. Section 6 concludes the paper.

2 Biomechanics of the human lower extremity

The user should feel the exoskeleton as a natural extension of his/her body; therefore, much attention should be paid to the design, biomechanics, and control aspects. Human

biomechanics are extensive and we cannot include everything in this short section. Instead, there are specific points that should carefully be considered:

- The number of walking phases and the kinematics parameters during one gait cycle,
- The motion range of the human joints,
- The joint behavior (it behaves like actuator, or damper, or even passive element),
- The timing of muscle activity patterns and synchronicity with the exoskeleton parts, and
- The effect of carried load on human body.

To end this, the following important subsections are summarized.

2.1 Gait cycle

According to Fig. 1, the human gait cycle can be divided into two walking phases [50, 51]:

- Stance phase, where one foot is in contact with ground, including 4 walking sub-phases: initial contact IC, opposite toe off OT, heel rise HS, and opposite initial contact OI,
- Swing phase, where one foot swings freely in the air, with 3 walking sub-phases: toe off TO, feet adjacent FA, and tibia vertical TV.

In view of the above, there are seven walking sub-phases during the whole gait cycle. As noted in Fig. 1, the configuration of human lower limbs and their relative position changes during the whole gait cycle, hence every walking sub-phase has its own dynamic modeling and controller. Accordingly, gait cycle division should carefully be considered while designing the control algorithm for the LEEs; selection of the suitable division of walking phases and the way at which they are synchronized are necessary for recreating a feasible walking pattern. For more details on walking patterns of biped robots and miscellaneous walking phases, see [22–26, 30]. This topic is briefly discussed in Sects. 4 and 5.

2.2 Lower limb motion

It is necessary to understand the way the joint angle positions of lower limbs are determined in Fig. 2. The knee angle can be defined as the angle between the femur and the tibia, it is clockwise positive (flexion) and counterclockwise negative (extension). Whereas the angle between the tibia and an arbitrary line along the foot refers to the ankle angle, it is normally 90°, but it is defined as 0° neutrally. The ankle angle is in plantarflexion if it is in a negative clockwise position and it makes dorsiflexion with a counterclockwise negative position. The hip angle can be defined in two ways: either as the angle between the vertical and the femur or as the angle between the pelvis and the femur [50]. According to Fig. 2, it is a positive clockwise angle with extension and a negative counterclockwise angle with flexion. The maximum range of sagittal motion of the hip is 110°-130° for flexion (larger range when knee is in flexion), and 30° for extension, whereas the knee has about 130° for flexion and 0°-maximum 5° for extension. The limits of ankle motion in the sagittal plane are 40° for flexion (dorsiflexion) and 20°

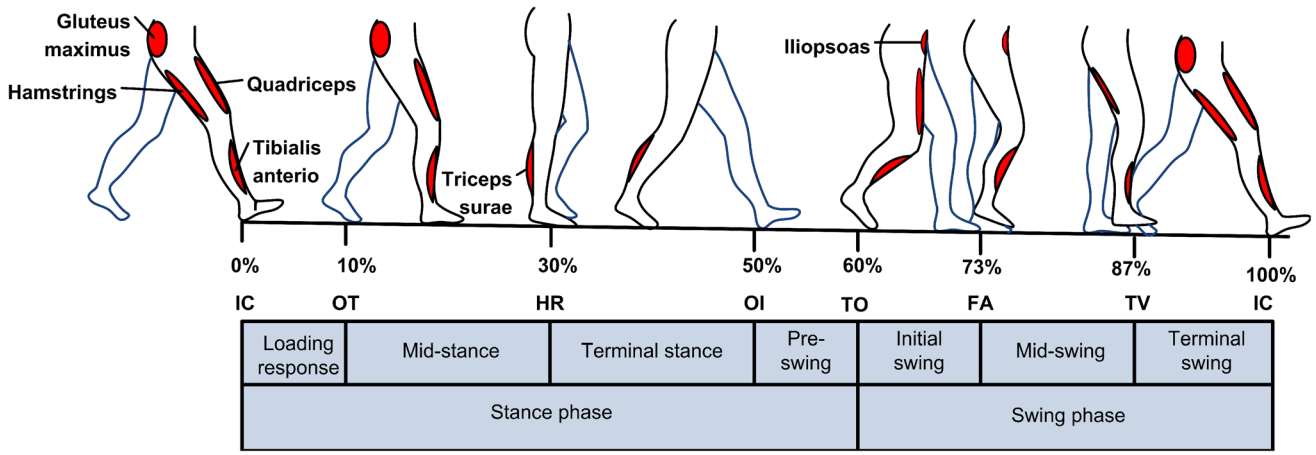

Fig. 1 Divisions of gait cycle with typical muscle activity patterns [50, 51]. The gluteus maximus and hamstrings are hip extensors. The hamstrings are active at the IC in order to prevent hyperextension of the knee. The quadriceps are knee extensors helping in control of knee flexion. The iliopsoas is a hip flexor and active during the initial and mid-swing phase. Tibialis anterior are active throughout the swing phase and the loading response in order to control the ankle plantarflexion during the loading response and initial swing and maintain the ankle dorsiflexion during the late swing phase. Triceps surae are active during late mid-stance and terminal stance in order to control dorsiflexion during the corresponding periods

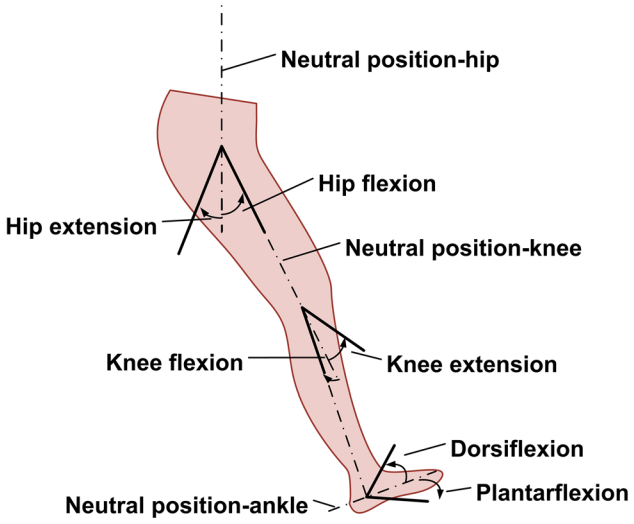

Fig. 2 Lower limb joints positions [50]

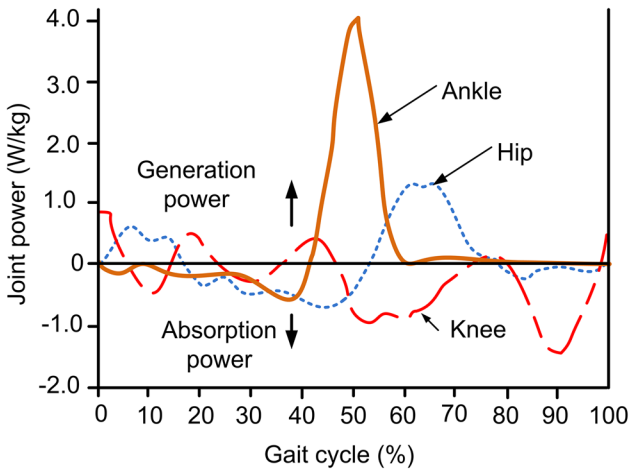

Fig. 3 Lower limb joint power during gait cycle [50]. The generation power at a joint produced when the joint motion moves in the direction of muscle action, while absorption power at a joint occurs if the joint moves opposite to muscle action

for extension (plantarflexion) [52]. The exoskeleton should not exceed the motion ranges of the user [6].

2.3 Behavior of lower limb joints

According to Fig. 3, the most power generated at hip joint belongs to the initial swing phase. The knee joint has almost negative power (absorption of power) during the swing phase. The highest power is generated at the ankle at the pre-swing phase. In view of the above, the followings are recommended:

- The hip has to be powered with a specific actuator able to facilitate initiation of the swing phase.
- There is inherent damping generated at knee level. In general, there are three possible designs for a knee exoskeleton joint [53]: passive, variable damping, and powered. The passive design is sensitive to the environmental disturbances. Variable damping knee requires a power supply to modulate the damping level, whereas, the powered knee provides non-conservative positive power during walking. A trade-off design of variable damping and powered knee is developed as proposed in [53] for irregular terrains.
- The ankle behavior can be expressed as a passive spring with released energy at pre-swing phase, see [54] for example.
- Most works concentrate on sagittal plane motion due to the large joint motions associated with this plane. Human pelvis performs movements in all three plans while walking.

In effect, Kim et al. [55] proposed that absorption of energy at the human joints level is necessary for supporting; therefore, they considered passive, powered and dissipative elements for each joint in order to imitate human power described in Fig. 3.

2.4 Muscle activity patterns

Although Fig. 1 refers to the typical case of the timing of muscles associated with lower limb joints during the gait cycle, these timing and synchronization can be different from person to person. In addition, for the same person, the pattern of muscles may depend on the fatigue level and on the walking speed [50, 51]. This is critically challenging in determining the possible muscle patterns for the user; this problem results from the redundant structure of the human body. This topic is discussed in Sect. 5.

2.5 The effect of the weight of backpacks

In effect, people who carry heavy objects on their back may suffer from risky problems especially at the lower region of the spine; the injuries may extend to the lower extremities [51]. Different biomechanical studies have investigated the effect of the weight of carried loads on kinetics, kinematics and muscle activity of the human body. The walking parameters such as step length and limits of joint motion, etc. are affected by the carried loads [56]. In addition, the carried load can influence the trunk and lower extremity muscles [57–60]. In summary, to reduce the stresses produced at specific parts of the human body while lifting some objects, the PEs can be a possible solution, when Pes addresses trunk, too; supporting trunk and lower limbs is essential in order to achieve lower levels of stress at the corresponding human body parts while lifting a load. Figure 4 shows the typical

muscle activity patterns of trunk and lower extremity while lifting loads.

3 Actuation

In general, there are different exoskeleton prototypes with different anatomy and actuation systems. As aforementioned, it could be impossible to mimic all DoFs of the human lower extremity since many design issues can be encountered. Increasing the flexibility and the DoFs of the lower extremity's exoskeleton may lead to instability and computational complexity problems which are hardly solved [6].

Clinical gait analysis data show that the highest power at the ankle, knee and the hip occurs in flexion and extension; therefore, most studies concentrate on sagittal plane motion only. The ankle and the hip joints demand positive powers that should be actuated whereas the knee power is negative which means that it can be modelled as a variable damper. The human body, however, needs some positive knee power during ascending stairs; therefore, this motivates the researchers to design actuated knee joint [6]. BLEEX [6, 39–41] has 7 DoFs at each leg with only 4 hydraulically actuated joints: 3 DoFs at the hip with 2 actuated DoFs in flexion–extension and abduction–adduction planes, 1 sagittal-plane actuated DoF at the knee and 3 DoFs at the ankle with 1 plantar/dorsiflexion actuated joint. The unactuated joints were equipped with steel springs and elastomer parts. Kazerooni and his colleagues [6] have found that rolling motion of the human hip is slow; therefore, they decoupled the abduction–adduction (rolling) hip joint from the control of pitch joints in the sagittal plane. HAL-5 [31–38] has a flexion–extension actuated joint with DC servomotors at the hip and the knee. The unactuated ankle joint is passively equipped with springs. HIT-LEX [42] has 14 DoFs with only 2 electrically actuated flexion–extension DoFs at the knee and the hip; the other joints are passive with specific springs. Whereas, MIT exoskeleton [2–5] is a sagittal-planar and underactuated mechanism with one DoF of the series elastic actuator (SEA) at the hip, one variable-damping DoF at the knee and one passive DoF at the springy ankle; there are other versions for this structure as proposed in [33]. In summary, the following points should be considered:

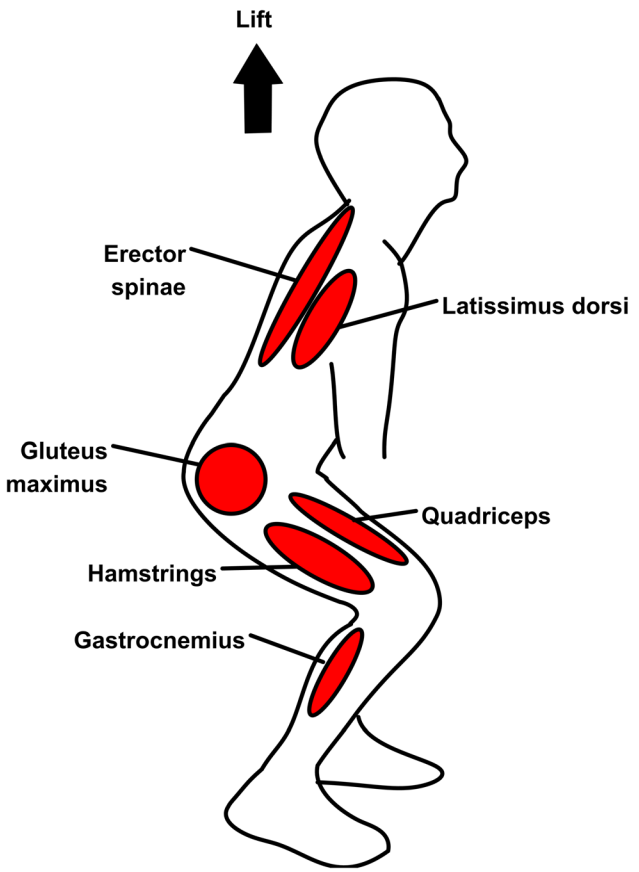

Fig. 4 The most typical muscle activity patterns while lifting some objects [51]. Accordingly, exoskeletons with supporting trunk and lower extremity are essential to relieve the corresponding muscles of the user

- Most designed actuators have currently some disadvantages such as large volume, heavy weight, high production of noise, high-energy consumption, etc. These actuators cannot be compared with human muscles that have inherent variable impedance characteristics. There are two options for the resolution of this problem: either a new design of the variable impedance actuators [61] or the use of active variable impedance control [62].
- Most researchers proposed actuated DoFs at the flexion–extension hip and knee joints with springy passive joints for ankle level. However, Herr and his colleagues [2–5] attempted to imitate the modeling of human joint by exploiting the variable damping at the knee, the controllable force actuation at the hip and the spring behavior of the ankle; their models are designed in sagittal plane only.
- Precise imitation of human anatomy could not be useful due to the accompanying complexity of the multibody dynamics and control. A trade-off design is necessary to be selected. A similar work is proposed in [55].

4 Dynamics

Humans have perfect mobility with amazing sensing, motor and control systems; being extremely versatile and adaptable, these systems provide smooth locomotion on all terrain. However, comprehensive understanding of the human locomotion is still not complete. To dynamically

model a biped mechanism, the following points should be taken into consideration [22, 29]:

- Biped mechanisms are mechanisms with kinematical variability such as they could be fully actuated during the single support phase (SSP) and over-actuated during the double support phase (DSP). If we assume the biped robot as a fixed-base mechanism, the dynamic modeling and control strategies of fixed-base manipulators can be used efficiently.
- Dealing with forward/inverse kinematics of the target LEE (if required) addresses different phases of the gait cycle. This may depend on the control architecture and the modeling complexity of the LEE. For example, a one-DOF LEE could not require forward/inverse kinematics algorithms or Jacobian transformation for control implementations. Another example is the impedance control of the LEE if used as a basis for control system of a multi-DOF LEE. The target impedance dynamics (outer impedance loop) is preferably expressed in terms of the task coordinate frames, since the task geometry may decide which directions are motion-constrained and force-sensitive [63]. In general, impedance control consists of two control loops: an outer impedance loop regulating the interaction between the end-effector and the external environment, and an inner control loop that can be a torque control loop or a position/velocity control loop. For an outer impedance loop, representation of the dynamics of the impedance target in terms of task space is necessary. For the inner control loop, there are two possibilities of coordinate representation for the control law. For force-based impedance control, the inner joint space torque control requires a transformation of the commanded forces generated by the outer loop into a commanded torque that should be tracked. Accordingly, this requires calculation of the Jacobian online. For the position/velocity-based impedance control (admittance control), the inner position/velocity control can be represented in joint space by transformation of the commanded task coordinates into joint coordinates using inverse kinematics [64–66]. However, the inner position/velocity control law can be represented in task coordinates, as presented in [67]. In effect, despite the usefulness of task space formulation for implementation of high-performance control schemes, measurement of the end-effector position and orientation (without the use of geometric Jacobian) is not easy; this may require vision technology. On the other hand, implementation of joint space control combined with a Cartesian impedance outer loop may require calculation of Jacobians and inverse kinematics schemes, which could be computationally complex [68]. See [69, 70] for more details on forward/inverse kinematics of lower extremity exoskeletons.
- Dealing with unilateral contact of the foot sole–ground interaction, we can approach this system as a passive joint model (rigid-to-rigid contact) or as a compliant model. However, for a non-disabled user, an underactuated ground-foot contact occurring during the gait cycle can be compensated by himself. Therefore, most manufactured exoskeletons with power augmentation did not offer any solution for this point, due to the computational complexity of the required dynamic modeling. On the other hand, if the LEE is simultaneously subjected to sudden impact, balance recovery should be considered even for a non-disabled user, bringing new challenges to the developers.

In view of the above, most exoskeleton researchers attempt to avoid using complete dynamics for the wearable robots. In effect, there are two general formulations for modeling the multibody dynamics: the Euler–Lagrange (E-L) formulation and the Newton–Euler (N-E) formulation. Although the E-L formulation can provide closed-form state equations suitable to advanced control strategies, their computational complexity, unless it is simplified, can be computationally inefficient for the analysis/control of the complex robotic system (more than 6 DoFs) [22, 29]. Whereas, the N-E formulation is a powerful tool to deal recursively with dynamics. The N-E-based virtual decomposition control (VDC) can be a good solution for dealing with the computational complexity associated with the dynamics and control of high DoF-robotic systems [27, 71, 72]. However, to our knowledge, most researchers focus on design of exoskeletons with just a few joints (e.g. the hip and the knee joints). Therefore, the E-L formulation has been used extensively in the literature; see Sect. 3 for more details on the design specifications of some manufactured exoskeletons. In general, there are two possible strategies for dynamics modeling of the LEEs: (i) the coupled exoskeleton-user dynamics, and (ii) the isolated dynamics of the LEE.

4.1 The coupled exoskeleton-user dynamics

This strategy attempts to model the whole dynamics of the coupled exoskeleton-user system. Accordingly, the interaction contact force wrench between the user and the exoskeleton at miscellaneous attachments disappears. However, this modeling is rarely used in literature. Consider the 1-DoF exoskeleton described in Fig. 5. According to the Lagrange formulation, the coupled dynamics can be described as [73, 74]

$$\left(I_r + I_h\right)\ddot{\theta} + \left(B_r + B_h\right)\dot{\theta} + K\theta + g_r(\theta) + g_h(\theta) = u + \tau_m + \tau_u \tag{1}$$

where $I_{(.)}$ represent the leg inertia with subscripts r and h being denoted to the exoskeleton and the user respectively, θ is the knee joint angle, $B_{(.)}$ is the joint damping coefficient resulted from friction effect, K is the knee joint stiffness of the user, $g_{(.)}$ is the gravity term, u is the input actuator torque of the exoskeleton, τ_m is the input control of the user resulted from the muscle effects, and τ_u is the unmodeled dynamics effect.

For Eq. (1), the following points should be noted:

- Although Eq. (1) includes viscous friction term, the modeling of the friction effect can be complex. In general, the friction torque can be expressed as a function of the relative joint angular velocity, see [22] and the references therein.

$$\begin{aligned}\boldsymbol{\tau}_f &= coulomb\ friction + viscous\ friction \\ &\quad + Stribeck\ friction + friction\ offset\ term \\ &= B_c\ sign(\dot{\theta}) + B_v\dot{\theta} + B_s\ sign(\dot{\theta})\exp\left(-\left(\dot{\theta}/\eta_s\right)\right) + B_o\end{aligned} \tag{2}$$

  where B_c, B_v and B_s denote the Coulomb friction coefficient, viscous friction coefficient, and Stribeck friction effect respectively, η_s is the rate of decay of the Stribeck friction, and B_o is the friction offset term.

- According to Eq. (1), calculation of the actuator torques of the exoskeleton may require knowledge (estimation) of the user input control, the un-modeled dynamics, and the user dynamics parameters associated with inertia, damping, gravity and stiffness. Robust and adaptive control structures are powerful tools to deal with this problem.

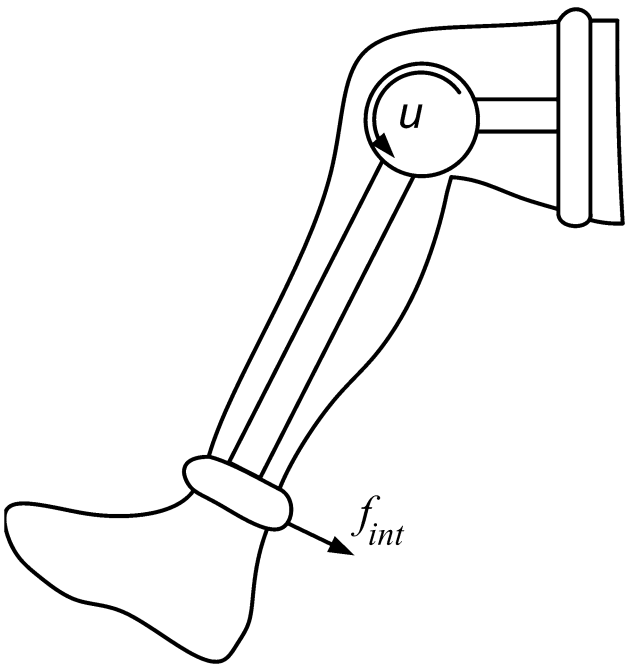

Fig. 5 The 1-DoF low limb exoskeleton at knee joint level [73]

In effect, even the LEE is a single joint one, the coupled dynamics should consider the whole user body dynamics. This is carefully developed in the work of Greggs and his colleagues [75, 76] in what concerns modeling multi-DoF coupled exoskeleton/prosthesis systems. For example, Lv et al. [76] decoupled the dynamics of swing and stance for each leg separately in a powered ankle–foot orthosis, taking the interaction forces of the two legs into consideration. The locomotion of the stance leg can be discretized into three walking phases: heel contact, flat foot contact and the toe-off contact, with the inertial coordinate frame selected on either the heel or the toe, according to the walking phase. For the swing leg, the hip is considered as the floating base, with zero interaction forces at the swing foot. Then the authors derived the equivalent dynamics with different support foot constraints that are important to design the underactuated potential shape control law. As noted, the dynamic modeling still requires transition times between walking phases and different sensors for determining the phase periods. Therefore, Gregg et al. [75] proposed a virtual constraint-based approach as a powerful tool to solve the transition problem. The virtual constraint approach has been applied to a biped robot in which the joint angles are represented by a monotonic variable that represents the walking phase. Please, see [77–81] for more details on this strategy. However, most virtual constraint-based dynamics assume that the investigated robotic system is an underactuated system that needs specific control strategies such as hybrid zero dynamics, post-Hamiltonian port approach, etc.

4.2 The isolated LEE dynamics

The subsection is focused on isolation the dynamics of the exoskeleton from the user and presents the effect of the user dynamics via the interaction contact force wrench generated at the attachments. There are two possible techniques for this strategy: (i) the coupled legs-based dynamics and (ii) the decoupled legs-based dynamics.

4.2.1 The coupled-legs-based dynamics

The coupled-legs-based dynamics means modeling of the biped wearable robot completely, to distinguish it from the decoupled-legs-based dynamics described at the end of this subsection. It includes selections of suitable walking phases and then modeling of the robotic system according to its configuration in the specific walking phase. This modeling strategy is extensively used in biped robots [21–30]. The PEs should decide the suitable time (period) for walking transition during the gait cycle. However, the main difference

between the dynamics of the pure biped robot and the LEE lies in the presence of the imposed constraints on the LEE due to the contact between the user's lower limb parts and the exoskeleton parts. The biped robot can be modeled as a robot in free space during the SSP, whereas the LEE is always in constrained space due to the interaction with the user. In view of the above, the gait cycle is divided into multi-walking phases with separate dynamics and control [75]. Kazerooni and his team [6, 39–41] proposed three walking phases for BLEEX: SSP, DSP, and DSP with one redundancy, see Fig. 6. The SSP (Fig. 6a) involves 7 DoFs within 6 actuated joints and hence the exoskeleton is an underactuated system. The E-L formulation for the LEE during the SSP can be written as

$$M(q)\ddot{q} + C(q,\dot{q})\dot{q} + g(q) = u + J(q)^T F_{int} \tag{3}$$

where $M(q)$ is the inertia matrix, q is the generalized angular joint displacement, $C(q,\dot{q})$ is the Coriolis and centripetal matrix, $g(q)$ is the gravity vector, u is the input control torque of the actuators with zero element at the ground-foot contact, $J(q)$ is the Jacobian matrix associated with the interaction force wrench vector F_{int} resulted due to the contact between the user and the exoskeleton at different places.

For modeling the SSP, the following important points should be considered:

- The problem of the underactuation associated with the SSP can be compensated by the healthy user [6, 39–41]. However, the elderly user can lose their balance during motion due to their vestibular deficits, weak muscles and reduced coordination capacity. Accordingly, the stabilization control strategies of underactuated biped locomotion should be used for elderly users. Different disturbed walking patterns associated to different pathologies requires different control strategies.
- The actuator dynamics is not considered in Eq. (3). However, consideration of actuator dynamics is important for a robot with high-velocity movement and highly varying loads. For more details on the effect of neglecting actuator dynamics, the reader is referred to [67]. In addition, the reader is referred to [67, 82–84] for more details on modeling of electro-mechanical, hydraulic, pneumatic, and flexible joint actuators, respectively.

Whereas the second phase is a DSP with two planar 3-DoF serial mechanism (see Fig. 6b), each leg has its own equation of motion. Accordingly, the E-L formulation for the left and right legs can be expressed as

$$M_L(q_L)\ddot{q}_L + C_L(q_L,\dot{q}_L)\dot{q}_L + g_L(q_L) = u_L + J_L^T F_{int_L} + \Phi_L^T F_{cL} \tag{4a}$$

$$M_R(q_R)\ddot{q}_R + C_R(q_R,\dot{q}_R)\dot{q}_R + g_R(q_R) = u_R + J_R^T F_{int_R} + \Phi_R^T F_{cR} \tag{4b}$$

$$F_{cL} = -F_{cR} \tag{4c}$$

where L and R refer to the left and right leg, respectively, $\Phi_{(.)}$ is a Jacobian constraint matrix associated with the coupling effect force wrench F_c resulted from splitting of the uppermost link (torso) into two parts.

It is recommended to transform Eq. (4) in terms of Cartesian coordinates. This is suitable for cancelling the coupling torque resulted from the partitioning process of the torso. Multiplying both sides of the above equations by the corresponding Jacobian inverse transposition, summing them and using the Newton's Third Law, it results in

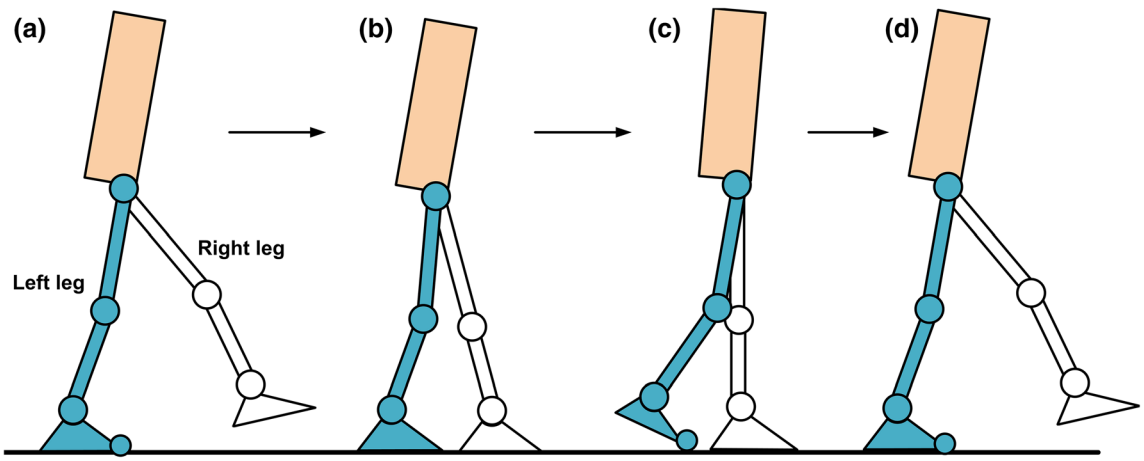

Fig. 6 The three walking phases proposed for Bleex [6]: **a** the SSP with joints described in circles, **b** the DSP1 with both feet on the ground, **c** the DSP2 with joint redundancy (left foot rotation), and **d** the SSP. It should be noted that the LEE has 7 DoFs with 6 actuators during the SSP and hence, the system is underactuated, whereas, the LEE is overactuated during both the DSP1 and DSP2. However, the decomposition of lower limb according to the approach described in [6] can result in different philosophy

$$F_{int} = J(q_L)^{-T}(M_L(q_L)\ddot{q}_L + C_L(q_L,\dot{q}_L)\dot{q}_L + g_L(q_L) - u_L) + J(q_R)^{-T}(M_R(q_R)\ddot{q}_R + C_R(q_R,\dot{q}_R)\dot{q}_R + g_R(q_R) - u_R) \quad (5)$$

The following important things should be considered for this walking sub-phase:

- Equations (4a) and (4b) include splitting the torso link into two parts such that the total torso mass m_T is equal to

$$m_T = m_{TR} + m_{TL} \quad (6)$$

where the two partitioned masses (m_{TR} and m_{TL}) can be calculated as

$$\frac{m_{TR}}{m_{TL}} = \frac{x_{TL}}{x_{TR}} \quad (7)$$

where x_{TL} is the distance of the torso center of mass from the left-ankle joint and x_{TR} is the distance of the torso center of mass from the right ankle joint.

- The whole exoskeleton system is an overactuated system, during the DSP; the number of actuators is equal to 6 while the LEE has only 3 DoFs. The system has an infinite number of solutions due to the inherent redundancy of the actuator. For dealing with actuator redundancy and kinematic constraints, see [22, 71] for more details. Knowing that the total interaction contact force wrench of Eq. (5) can be distributed arbitrary to the left and right legs of the LEE; there are 3 redundant unknowns that can be solved using optimization techniques.
- The constraint equation of motion for the LEE developed for the DSP can be represented for the whole system without the partitioning process as described in [22] and the references therein. Accordingly, Eq. (3) can be used for modeling this walking phase (the DSP), but with F_{int} including the interaction contact force wrench plus the ground reaction forces (in case of an exoskeleton with supported feet). Equation (3) can be solved using two well-known techniques [22, 29]: the redundant coordinates-based technique which is mainly used in commercial software such as MSC ADAMS, and the minimum coordinates-based technique which could be, to some extent, suitable for control strategies and real-time applications. Many researchers have preferred the first technique due to its simplicity and ease of derivation at the expense of difficulties of the numerical methods encountered in the solution. Consequently, this motivates the researchers to investigate the second technique that includes eliminating the constraint equations (Lagrange multipliers) from Eq. (3) to result in constraint-free differential equations. This can be implemented using one of the methods of orthogonalization which are: the coordinate partitioning method, the zero-eigen value method, the singular value decomposition (SVD), the QR decomposition, the Udwadia-Kabala formulation, the PUTD method, and the Schur decomposition. See [22, 29] for more details.
- Regarding the actuator's dynamics see the above bullet list on the SSP.

The last phase of the gait cycle is a DSP with one redundancy source due to the rotation of the rear foot (see Fig. 6c). Kazerooni and Steger [6] has used the partition strategy for the torso in order to provide dynamics modeling for the LEE. According to their analysis, the left leg is underactuated due to one coordinate redundancy at the left foot, while the right foot is fully actuated. In effect, this modeling is unrealistic since the whole LEE system is still overactuated. The system has 6 actuators and 4 DoFs and hence 2 redundant coordinates are produced. This point is well dealt in [9, 22, 71].

In DSP1, both the rear and front feet are in full contact with the ground, whereas DSP2 includes the rotation of the rear foot about the toe joint with front foot in full-contact.

The difficulties associated with this strategy are [75]:

- The time of each walking phase should be determined; the wrong estimation of the walking phase periods may result in imbalance problems due to the interference of the walking phases.
- The tuning of the control parameters (gains) is not trivial for multi-models during the gait cycle.
- Designing an LEE with attachments under the feet rise inherent dynamics and control problems, due to integration of the ground reaction forces and the interaction force wrench resulted from the user during the support phase. Differentiating between these two forces is necessary in order to assure stability during motion; see [9] for more details. This can be avoided by making the attachments at the legs as proposed for some prototypes; see for example the design of [85]. Due to the difficulties associated to this dynamic modeling, most manufactured exoskeletons avoid this approach and attempt to propose a model-free control algorithms, e.g. used decoupled joint control, without the need for complete a dynamic modeling.

4.2.2 Decoupled legs dynamics

This technique deals with dynamically modeling of the swing and support phases for both lower limbs considered separately, without considering the coupling effect between the two lower limbs. The researchers attempted to compensate for this modeling error by using a robust controller for the whole system. Yang et al. [16] adopted this strategy for modeling LEE (see Fig. 7). Accordingly, each leg has two phases: swing and stance phases reducing the multi-models

proposed in subsection 4.1. However, the dynamic coupling between the legs was neglected in their proposed model. In effect, the coupling between the legs should carefully be considered since the proposed control architecture may depend on each leg dynamics, leading to gait errors and instability issues. Mathematically, the dynamics of each lower limb during the swing and the stance phases of the gait can be expressed as a fixed-base robotic manipulator with constraints at different locations due to the exoskeleton and its contact points with user's body parts. A similar equation to Eq. (3) can be used for both lower limbs, being in stance as well as in swing.

A similar technique is used in [76] but considering (i) the coupling effect of the two lower limbs, and (ii) the user dynamics.

As mentioned previously, it is important to consider that the decomposition of the biped walking can produce a false control law during the DSP, unless the overall stability of the system is ensured. Consider the DSP described in Fig. 6b, the one with 6 actuators and 7 generalized coordinates. The whole system has 4 DoFs and 6 actuators with 2 redundant generalized coordinates. Therefore, the system is overactuated with possibly infinite input control torques. However, decomposition of the LEE legs without considering the overall system constraints, as proposed in [16], may lead to false dynamics formulations. The left lower limb in Fig. 6b may consist of 4 DoFs with 3 actuators, while the right lower limb is fully actuated, which is unrealistic.

Zhu [71] has decomposed a 5-link biped robot during a complete gait cycle with ensured stability. The biped robot is underactuated during the SSP, with 4 actuators and 5 DoFs.

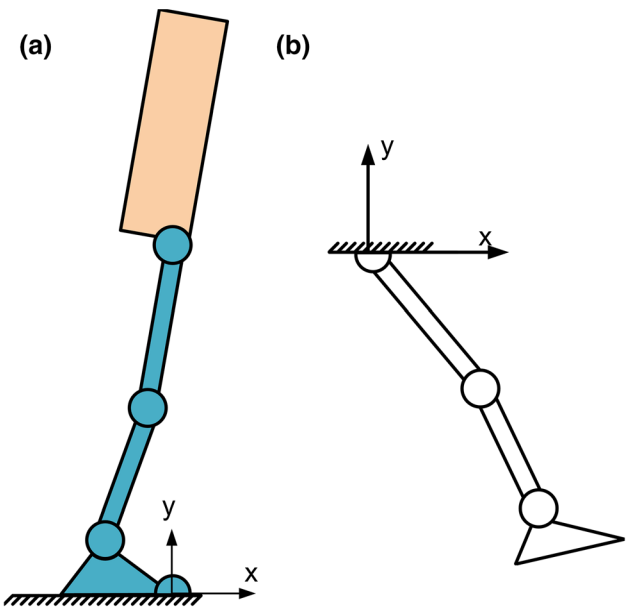

Fig. 7 The dynamics modeling for the LEE [16]: **a** the stance lower limb, and **b** the swing lower limb

The author has used a time-scaling control approach in order to deal with the underactuation issue. Whereas, the biped robot is overactuated during the DSP, with 4 actuators and 3 DoFs. An optimization technique has been used to deal with the overactuation problem and to release the underactuated joints of the feet. Thus, despite of the decomposition approach, the stability of the overall system is guaranteed.

In general, the LEE is a floating system and it is hard to assume that the hip is fixed for modeling the SSP. Dynamical decomposition of robotic or exoskeleton systems requires considering the whole system constraints, otherwise the analysis is not feasible.

Remark 1 The control architecture of HAL-5 includes decoupled PD tracking control and phase synchronization for each lower limb, separately, without the need for formulation of dynamic modeling of human–robot interaction [31–38] HAL has the advantage of a real-time input from the sensors indicating to the exoskeleton's actuators the movement intentions of the user's lower limbs. The HIT-LEX [42] is also a model-free controlled exoskeleton; its control architecture includes speed control of each joint with outer impedance control. The control system of the MIT exoskeleton [2–5] also avoids using the dynamics of the exoskeleton and the user. It should be noted that most dynamic modeling-free control systems are decentralized independent joint control systems using synchronization of the walking phase periods [75]; the details of a control system for lower extremity exoskeletons will be described in next section.

5 Control algorithms

Since the exoskeleton robot is an auxiliary robot in direct contact to the user, three important points should be considered while designing the LEE:

- Power assist rate. The wearable robot should follow the intended human motion carefully without interference and providing auxiliary energy when needed [1].
- Minimization of interaction force wrench. The control algorithm should ensure the exoskeleton move together with the user, with minimal interaction forces [6].
- Estimation of interaction force wrench. As aforementioned, the exoskeleton robot can be connected to different regions of the wearer's body, imposing uncomfortable interaction forces/torques to him/her. The proposed controller for the user-exoskeleton interaction is preferred to consider the locations and the values of the interaction forces to be unknown; this makes the control architecture more robust and non-sensitive to any unpredicted disturbances.

There are miscellaneous control algorithms for controlling and regulating the human–robot interactions in PE systems, however, the general architecture of control strategy could consist of loops of three levels of control (see Fig. 8): a high-level control strategy that is responsible for estimating the walking intention, mid-level control that decides the switching rules between the walking phases, and low-level control that stabilizes the human–robot interaction, e.g. position control, impedance control, etc. Fewer attempts have been made to use one level control strategy for control of LEE except for work of Kazerooni and his colleagues [6, 39–41].

5.1 High-level control

As aforementioned, the high-level control includes capturing the human walking intention that is tracked by the exoskeleton actuators (low-level control). There is no direct technology that can estimate the human intent. The bioelectric sensors that estimate the angular joint variable states can provide indicators for estimation and observation of human walking intention [31, 32]. Sankai [31] proposed that bioelectrical sensors used in Electromyography EMG can successfully detect the healthy user intention; however, the obtained sensor readings can be of no value in people with gait and ambulation disabilities due to neurological conditions. The authors proposed to use the center of gravity (COG) shift as indicator for gait movements intention, as a substitute for the EMG signals since the COG shift is more reliable compared with muscles activity-based bioelectrical signals. Kazerooni and his colleagues [6, 39–41] designed the control system for BLEEX without any measurement from the user. Pratt et al. [7] has used the knee joint angle and the ground reaction force as indicators for the user intention. Deng et al. [86] used four 2-D force sensors at the interaction places on thighs and shanks and two force sensors under the soles for motion acquisition from the user lower limbs. Based on multibody dynamics and on measured interaction forces, the interaction output torque can be estimated. The 6-D force sensors were used extensively for detecting human walking intentions for lower limb exoskeletons at specific locations of interactions such as the feet and the back; please see [87–91] for more details. In view of above discussions, the methods for determining the user intention can be classified as follows: method based on the EMG technique, method based on body's global kinematics, method based on interaction force measurement

5.1.1 EMG-based method

The exoskeleton is an extension of the user's body and it may require a direct connection to the user's nervous system. However, this connection should be easily attached, harmless and as less invasive as possible [7]. In addition, the goal of the exoskeleton is not only to augment power user's power, but also to support and share intended motions. Accordingly, the exoskeleton is preferred to exhibit bio-inspired performance [62]. One of the effective methods for estimation of the human motion is the electromyogram EMG technique. The myoelectrical signal of the muscle is related to the muscle torque; the relationship can be linear [38]. Therefore, the assist force/torque required to support the user can accordingly be determined. The myoelectric signal collectors are attached to specified regions of the user's skin. These signals are always noisy and should be amplified and filtered [38]. Kawamoto and Sankai [38] used EMG measurements to estimate the assistive force/torque required from the exoskeleton actuators (hip and knee joints). The authors selected specific locations to place their EMG electrodes, as described in Fig. 9. The bioelectrical signals were amplified

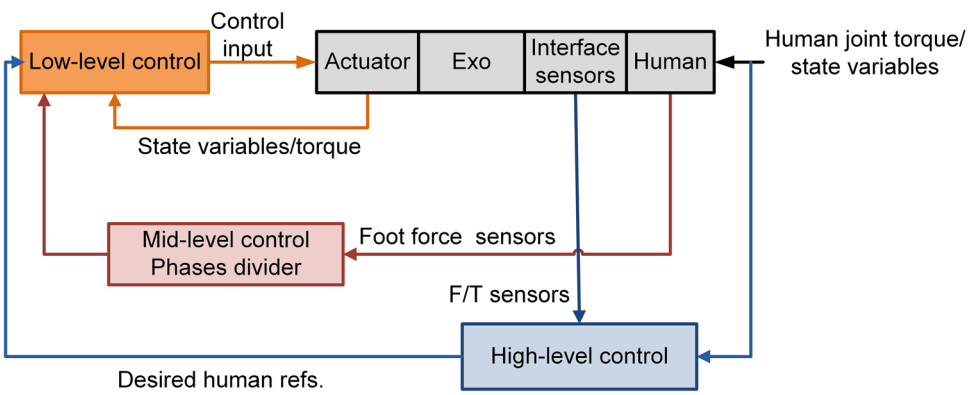

Fig. 8 A general control architecture for stabilization motion of the LEE. The high-level control is responsible for estimation of the desired human motion references, joint torques, leg stiffness, etc. The mid-level control is a regulator for determining the switching periods of the walking phases. The low-level control can be pure position control, impedance control, etc. It is responsible for motion stabilization of the coupled user-exoskeleton system

and filtered and transferred to a PC for further processing. The authors found that there is a linear relationship between the joint torques generated by the corresponding muscles and the measured EMG signals. A calibration technique based on least squares was used for determining the required control parameters.

On the other hand, Kiguchi and Hayashi [52] used EMG-based control for extracting the human walking intention. Root mean square is used for extraction of the raw EMG signals that are placed at 8 locations. In their exoskeleton, the ankle is actuated, therefore, the distribution of the electrodes is different from that on the HAL exoskeleton. They used a neuro-fuzzy (N-F) modifier in order to process the motion intention of the user based on the interaction force sensors. The input to the N-F model is the joint angles (hip, knee and ankle angles) and the output is the weight matrix that correlates the estimated torque to the sensed EMG signals. The key idea is to train the neuro-fuzzy model modifier such that the weight matrix of the calibrated EMG signals are defined perfectly. If there is a deviation between the user motion and the exoskeleton motion, the force sensors detect (measure) the interaction forces between them and N-F model attunes the weight matrix to cancel these forces. The authors used impedance control as a low-level control for generating the required actuator torques of the exoskeleton. In general, the stages of processing the EMG signals and commanding them to the low-level control can be described in Fig. 10.

Generally, EMG-based human walking intention could have some limitations [9, 52].

- It could be uncomfortable for daily use due to the attached electrodes on the skin.
- The obtained EMG signals can be different for the same muscle and motion and even for the same user; the relationship between the joint torque and the measured EMG signals are not unique.
- To get more accurate joint torque estimate, the activity of the muscle groups mobilize the joint should be sensed by EMGs.
- It is not easy to determine the weight matrix relating the myoelectrical signals and the torques generated by the muscles, due to the postural differences of the lower limb; the moment arms change in accordance to the joint angle.
- The muscle has contractile and passive elements, whereas, EMG signals can sense the muscle activity associated with the contractile elements. In view of above, a combined mechanical model and EMG control is necessary to get an optimal estimation for the joint torque value.
- Raw EMG signals are very noisy and should be filtered (extracted) for control purposes such as low pass filter, root means square, mean absolute value, etc.

Remark 2 The output of filtered EMG signals is represented by the estimated joint torques developed by the user. The estimated torques can be transformed to end-effector forces (at the feet in the case of LEE) by using Jacobian

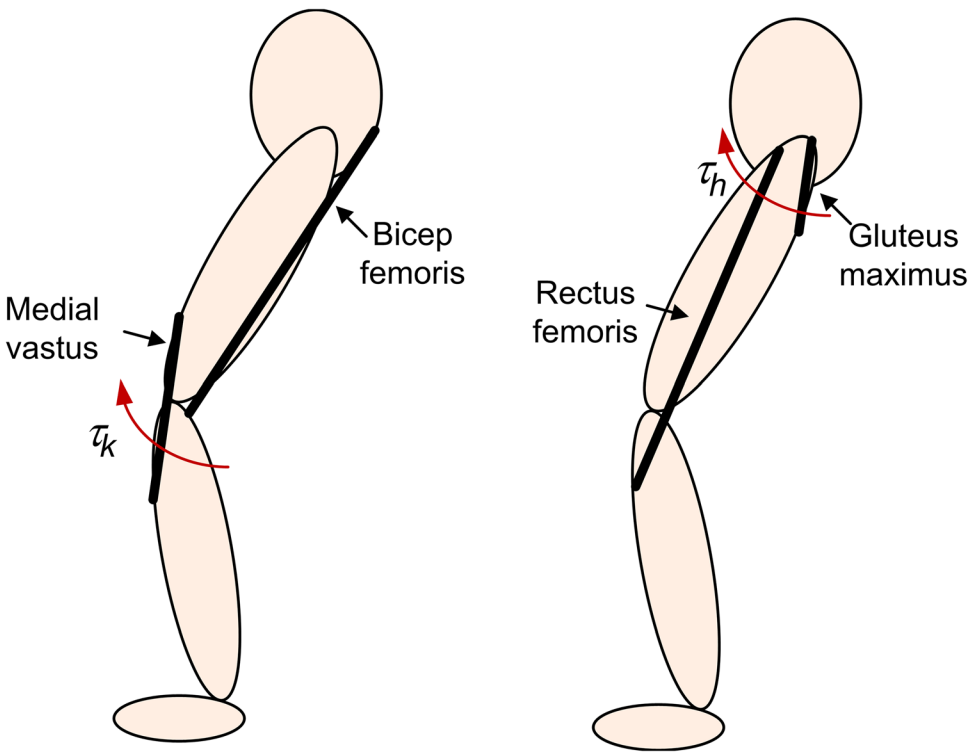

Fig. 9 Description of major muscle ligaments affected on hip and knee joint torques, τ_h and τ_k respectively [38]

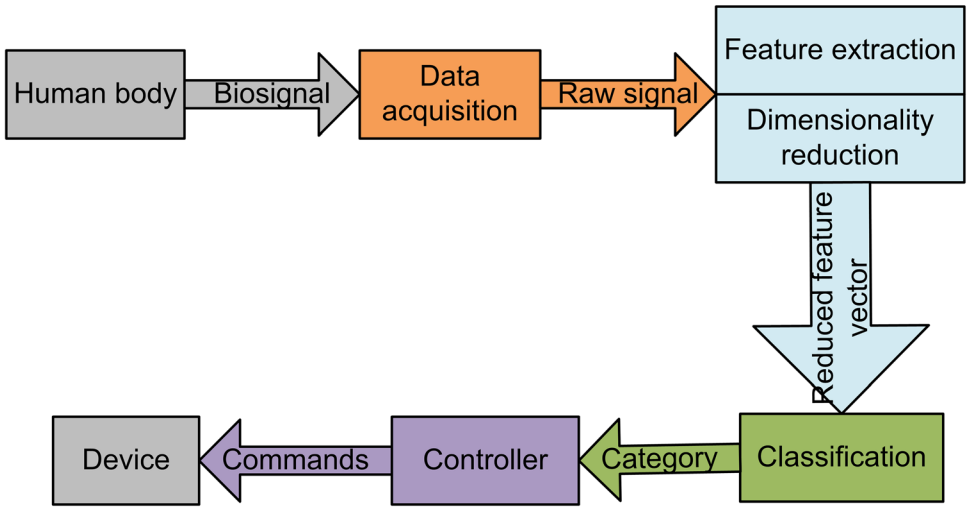

Fig. 10 Processing stages of EMG-based control architecture [121]

as proposed in [52], then the role of low-level control, e.g. impedance control comes. However, the filtered EMG signals can be transformed into the corresponding joint angles by using a linear relationship between the infinitesimal change of the estimated joint torques as emphasized by the filtered EMG and the infinitesimal change of corresponding joint angles, please see [92, 93] for more details. Then any position controller can be used as a low-level control for tracking purposes. Winter [94] described a schematic diagram for analyzing human motion. The schematic diagram consists of two stages: muscle model stage with two inputs of EMG signals and output consisting of neural stimuli and force wrench, and link segment model with force wrench as input and variable states of human links as output, see Page 6 of [94].

Remark 3 Due to the explicit relationship between the joint stiffness and the joint torque, the EMG can be equivalently used for estimation of the user stiffness. Please see [62, 95, 96] for more details.

5.1.2 Global kinematic parameters

According to biomechanics, there are four techniques in order to define the global trajectory of the nonlinear walking and to estimate the next walking step: the footprint trajectory, orientation of pelvis, orientation of torso and the head [97]; most of them could be connected with the centre of gravity (COG) position. Estimation of COG in lateral plane can be a good index for walking transition from DSP to SSP. There are different techniques for measurement/estimation of the COG position/trajectory as follows.

- The measurement of COG can be approximated by placing the accelerometer on the pelvis. In effect, the pelvis trajectory is linked to the actual orientation of the body and could be a strong index for some human walking tasks [97]. The velocity and the position of the COG can consequently be deduced. There are two limitations when using accelerometers: the noise disturbance of acceleration measurement and the demand for knowledge of the initial velocity and of the position of pelvis for integration techniques [97].
- There are other techniques for estimation of COG position such as walking treadmill, the step frequency combined with constant step length. Recording the step length and width for nonlinear walking is not straightforward and is difficult to be estimated.
- The model of inverted pendulum is extensively used for detecting the COG trajectory, please see [22, 24, 30, 98] for more details on this technique.
- A powerful technique for estimation of the COG acceleration is to use force plate under the foot in order to measure the ground reaction forces [31, 32, 97]. Using simple dynamics, the acceleration of the COG can be estimated, see [22, 24, 30, 97] for more details.

However, people with gait disorders may present reduced muscle force and lack of balance, such the COG position could be improperly estimated. Consequently, the torso position could be alternative tool for this problem. The torso configuration can be alternative tool for human intentions for user with weak muscles. A gyroscope box could estimate three possible rotational angles of the torso by integrating the measured angular velocity of the torso. The head orientation combined with the torso orientation can also be strong indication for predicting the next walking step [97, 99]. The head has unchanged acceleration profile despite walking on uneven terrains and different gait cycle pattern [97, 100].

Remark 4 Since the power assist exoskeleton should work in daily life, the designer should have in mind that the user's intention is preferred to be captured online; this makes the human–robot system robust to unexpected conditions and disturbances. In effect, there are other measurement methods for sensing and capturing the global human walking parameters, e.g. visual markers and functional approach for measuring the joint displacements, and the magnetic or inertial capture systems for sensing the joint angles, etc. The traditional human motion tracking methods depend on complicated high-order calculations for capturing human kinematics [101]. The reader is referred to Chapter 8 of [97] for more details on these approaches. However, much attention has been paid to the wearable Inertial Measurement Unit (IMU) systems due to their portability and high accuracy even for use in unstructured environments [101–105]. Units consisting in accelerometers, magnetometers, gyroscopes, provide easy and quick measurements. They allow clinicians and researchers access to data regarding important spatial–temporal parameters: gait speed, cadence, step length, stride length, gait cycle duration, stance and swing phase duration, double and single support duration, angles of joints during gait cycle, and give the possibility to obtain important information regarding gait variability, predictor of physical and cognitive deterioration [106–109]. In addition, lightweight, flexible systems capable of detecting mechanical parameters as strain and pressure are in research and development lately for gait analysis [110].

Remark 5 In effect, high-level control can include hybrid strategies (hybrid multimodal-interaction platforms) for capturing the user intention, e.g., Lenzi et al. [8] used force sensors under soles and mechanical goniometers for estimation of kinematic parameters of the user. Cifuentes and Frizera [111] used a novel sensor fusion method that includes: (1) a laser range finder sensor for estimation of user's leg kinematics, (2) inertial measurements units for estimation of orientation of parts of the coupled system of the user and the machine, and (3) triaxial F/T sensors for estimation of interaction force wrench at physical interaction between the user's upper limbs and the machine.

5.1.3 Interaction force measurement

The key idea of this method is to measure the interaction forces at specified locations and then to use Jacobian or impedance control principles to determine the user walking intention. The force sensors represent the interface between the user and the exoskeleton. It is undesirable to select the contact points between the user and the exoskeleton along the legs (thigh and shank) due to the accompanied sensitivity of the user for these locations during long walks. Accordingly, the more suitable choice for interaction contact is the sole of the foot, where the user is accustomed to feel the ground reaction forces (GRFs), and the back where the load can be distributed and isolated. However, the sensed net force under the user's feet consists of both the GRFs and the human–machine interaction forces (HMIFs). Therefore, differentiating between these two forces is necessary in order not to affect the motion of the user and not to increment possible instability problems. For heel strike, it is possible to differentiate between the ground reaction force GRFs region and the HMIFs region. However, the differentiation process could be difficult for feet in flat contact. In effect, it can be proved that the machine GRF is a scaled version of the human GRF for guaranteeing minimized interaction force wrench and suitable synchronization, see [9] for more details. In summary, measuring the interaction forces/torques poses some problems:

- The contact interaction locations are not known in advance and may vary accordingly. In other words, the user may prefer to put braces at the shank or/and at the thighs, etc. Measurements of these interaction forces/torques could be suitable for experiments rather than for a daily life use.
- Some exoskeletons have force/torque sensors at the feet of the user, however, the obtained sensor readings do not only represent the interaction forces/torques; the stance load can augment the values of these readings.
- Installation of force/torque sensors under the sole may lead to heavy feet. Besides, human walking consists of cyclic motions, which may induce irritation, fatigue, stresses at sensor level and even sensor failure.

Ishida et al. [90, 91] used the measurement of the interaction force at the handle for extracting the data related to the motion of the user. Using the impedance control principle, the desired acceleration of the handle can be calculated. Twice integrating the desired acceleration and by using point-to-point control, the human–robot interaction can be stabilized. Zhang et al. [42] exploited the same technique for extracting the user motion for HIT-LEX exoskeleton. The force sensors are installed on the back of the user and under the feet. A similar technique has been used in Body Extender of PERCRO laboratory of Scuola Superiore Sant'Anna [87, 88]. Six-DoFs force sensors were installed in five locations of the user: the legs, the arms, and the back. Lenzi et al. [8] used two control levels for stabilization and control of a 1-DOF powered exoskeleton called ALEX II. The high-level control attempts to obtain the normalized hip torque as shown in Fig. 11.

Table 1 describes the features and limitations of high-level control strategies.

Remark 6 For a user with a gait disorder, the bioelectric signals transferred through the user body could be broken and improperly estimated. However, these signals are powerful for the non-disabled user and could be considered as reference walking patterns. Kiguchi and Hayashi [52] used two strategies for controlling and capturing the human walking intention for power-assist exoskeletons: power-assist control and perception-assist control. The power-assist control is based on EMG signals, and this part is effective if the user has no gait related disability, whereas the perception-assist robot includes modification of the user walk pattern based on intelligent approximator. A balance control strategy is necessary to compensate for the walk modification of a user with a gait disorder; healthy persons can compensate for the walk modification by themselves. A similar concept was used in [31–38].

5.2 Mid-level control

As aforementioned, the gait cycle consists of multiple phases with specific transition times. Accordingly, this control level is responsible for smooth transition between walking phases during the gait cycle. Due to the short time of DSP, some researchers concentrate on the SSP without considering the coordination control of the legs during walking. In effect, the strategy adopted for coordinating the walking legs is mainly based on the GRF at the sole. As a result, the GRF-based state machine strategy is a powerful tool to deal with synchronization and transition problems. Kazerooni [6, 39–41] used feet sensors to determine the three walking phases they proposed and which of the dynamic modeling method/algorithm they can apply. In HAL-5, the authors proposed inequality for ensuring stable transition times. For example,

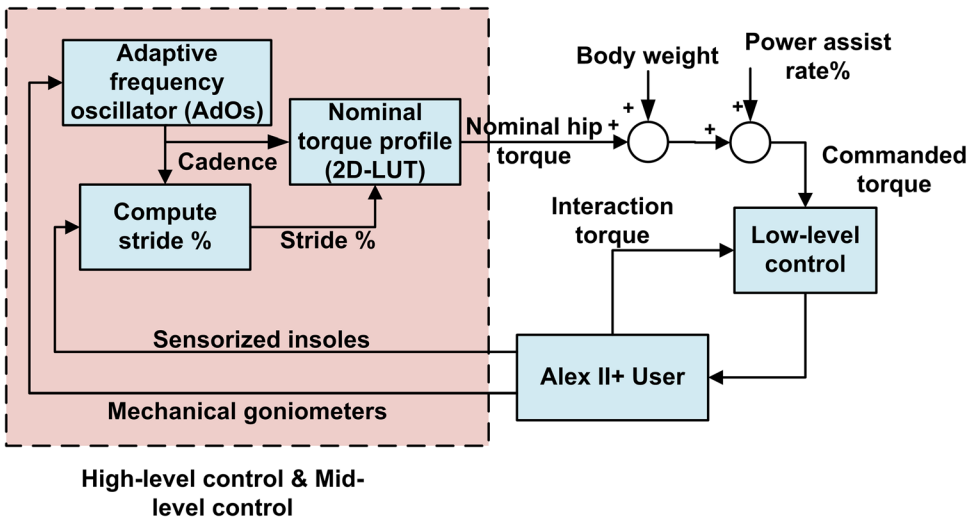

Fig. 11 The high-level control of Alex II that estimates the desired hip torques based on multi-stages [8]: the walking stride is computed based on GRF sensors under the sole, the adaptive frequency oscillator AdOs is used for estimating walking cadence, the nominal hip torque profile is determined from a bi-dimensional lookup table and the values of cadence and stride, the last stage includes adding the body weight and power assist rate to get the desired hip torque

Table 1 Features and Limitations of High-level Control Strategies

Control strategy	Description
The EMG-based Technique	It is a powerful bio-interface strategy for estimation of the user muscle activity, and hence the joint torque or the leg stiffness can be estimated The muscle biomechanical model is preferred to be integrated with the EMG technique for modeling of the passive and the contractile elements respectively The EMG signals require a multi-stage process for processing and acquisition of the useful data; see Fig. 10 Although some researchers attempt to avoid using the EMG technique, it can be necessary for verification and validation of the LEE platform
Global kinematic parameters	It includes kinematic measurement of the user motion such as the COG trajectory, joint angle trajectory, trunk trajectory, leg trajectory, etc. Different measuring methods for sensing and capturing the kinematic walking parameters such as visual markers, functional approach, the magnetic/inertial capture systems, laser range finder sensors, etc. If the designer attempts to use an interaction force observer, he/she may resort to determine the global kinematic parameters of the user for its importance in the low-level control. See Section III of [30] for more details
The HRI F/T sensors	It is useful to capture the user motion by sensing the HRI at some specific attachments The direct/indirect F/T control can require F/T sensors Due to the possible problems associated with practical implementation, a force observer is recommended. However, the force observer may require measurements of the state variables of the user that could not be straightforward

the right foot becomes support foot while the left foot will swing if the following inequality $f_r > f_l$, where $f_{(.)}$ is the ground reaction force at the right or left foot, is satisfied and vice versa. For more details, the reader is referred to [2–5, 42, 112].

5.3 Low-level control

As stated previously, low-level control aims to: (1) add power assist rate to user, (2) minimization of HIFMs as possible, and (3) tracking the desired torque/position using conventional control methods, e.g. PID family control, sliding mode control, etc. However, some researchers consider all these points in their control architecture but for a single joint exoskeleton design, e.g., only knee or hip orthosis, etc. In effect, the user-exoskeleton system is a biped constrained system with interaction force wrench at specific locations of the user lower limbs. The force control strategy is widely applied for robots in contact with the external environment. In general, the robot force control can be classified as [113]: Indirect force control such as compliance and impedance control, and direct force control such as hybrid force/position control with different versions. In view of the above, there are three possible approaches described in the following subsections.

5.3.1 Control approach 1

The key point in controlling and stabilizing the LEE is to regulate the interaction force wrench. This control approach includes tracking the user's references carefully or tracking null interaction force wrench. Consequently, pure position control or regulation of direct force/torque control can be used in accordance with this control point of view. To motivate the analysis, consider a 1-DoF LEE with dynamics shown in Fig. 12.

According to Fig. 12a, the following points can be noted:

- The input to the exoskeleton dynamics is represented by the actuator torques and the human–exoskeleton interaction torque.
- Although the attachment dynamics is modeled as stiffness, it can be modeled using impedance control principles with time-varying parameters as inspired by human behavior. As a result, the human–machine interaction torque can be determined as

$$\tau_{int} = K_h(q_h - q) \tag{8}$$

- If the force/torque (F/T) sensors are used to sense the HRI, Fig. 12b is proposed for experimental implementation. In effect, Fig. 12a is useful in simulation studies provided the impedance mode at interaction points is known.

According to Eq. (8), the target of the control algorithm for human–exoskeleton interaction is to make $\tau_{int} \to 0$ or equivalently $q_h \to q$. This means that the user does not feel loads carried by his/her back with more comfortability. Although this strategy is simpler in concept and attempts to avoid directly adding the required assistive power, it is expensive in terms of high actuator torques that can be required for the wearable exoskeleton. Following the work of Racine [9] and neglecting the nonlinearities associated with target system, PD control with inverse model can be used for control as shown in Fig. 13.

The transfer function $\left(\frac{q}{q_h}\right)$ can be determined as

$$\frac{q}{q_h} = \frac{K_h G}{1 - K_l + K_h G} \tag{9}$$

If $K_l \to 1$, then $q_h \to q$ and $\tau_{int} \to 0$.

See Chapters 6 and 7 of [9] for more details about modified versions of this control strategy, stability and performance.

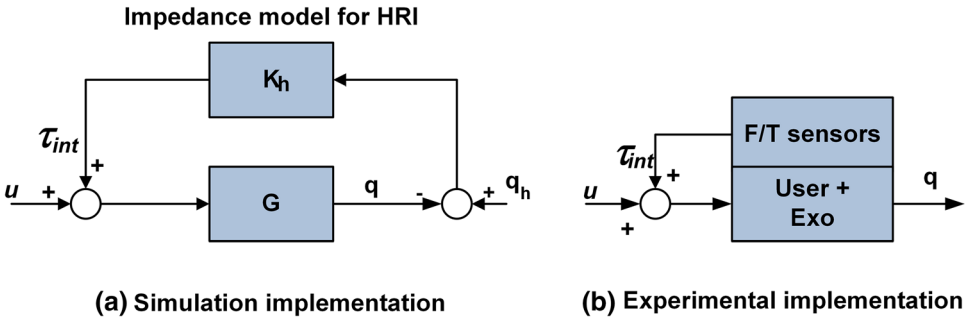

Fig. 12 Dynamics of human–robot interaction [9]. Although K_h represents user stiffness at the interaction locations, it can be extended to include impedance model with time-varying parameters. G signifies the exoskeleton transfer function, q is the angular position of exoskeleton joint, q_h is the angular position of the user, τ_{int} refers to the human–robot interaction torque, and u is the input control

Duong et al. [114] decomposed the stance and swing legs separately and proposed position PD control for stance leg and virtual torque control with radial basis function approximator for the swing leg. It is a hybrid control aiming to precisely tracking the user motion, making interaction force wrench approximately null or very small. Handiman exoskeleton [6, 14–16] was designed and controlled based on master–slave control. It consists of two overlapping exoskeletons with an inner skeleton in contact with the user. The idea is to manipulate the master inner exoskeletons by the user in order to control the slave outer exoskeleton. This strategy includes tracking the user angular joints or the torso displacement and capturing the whole user motion [9]. There are two problems associated with master–slave control architecture: the limited space between the user and the overlapping exoskeletons that is necessary for installing the instruments, and imitation of all motions of the user that can lead to uncontrolled actions [9]. Sankai and his colleagues [31–38] used decoupled PD position controllers to control the pitch angles of the hip and the knee of HAL exoskeleton with desired angular references extracted from foot sensors-based user intention estimators, see Fig. 14.

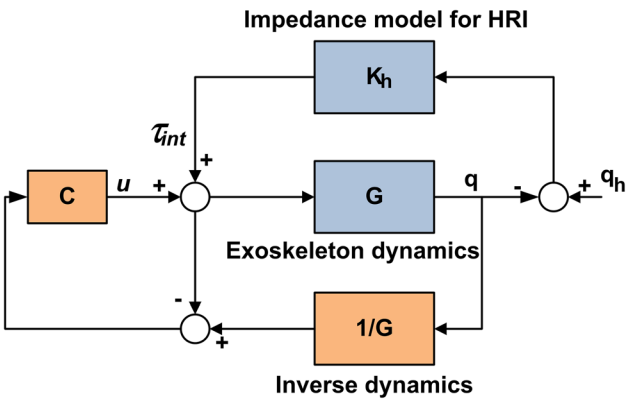

Fig. 13 A simple control architecture for LEE based on conventional controller C and inverse dynamics of the host system [9]

Racine [9] exploited the strategies of direct force control [113] and applied it to the PE. The key idea is to make the user does not feel the exoskeleton enhancing comfort. Figure 15 shows the proposed controller for 1-DOF exoskeleton joint, see Chapter 7 of [9] for more details. However, tracking null interaction torque references can be undesirable because some value for the interaction force are needed due to its importance in extraction of the user intention.

Zanotto et al. [115] used two torque control strategies for LEE with two powered joints at the hip and the knee. Figure 16 shows the two control approaches in one schematic diagram with control selector for switching purposes. The outer torque control is based on installation of force/torque sensors at the interaction location between the exoskeleton and the user, whereas the inner torque control includes installation of torque sensors between the actuators and output load (gearbox output shaft) with feedforward friction and gravity compensators. The interesting point is that the torque feedback with torque sensors at the output shaft only reflects the inertia of motor and gearbox whereas the user is responsible for compensating for the remaining exoskeleton dynamics, i.e., links. This is not the case for torque control with force/torque sensors at the interaction locations where the exoskeleton dynamics is masked by feedback torque control.

Despite the importance of the measurement of interaction force wrench in control architecture for PEs, there can be practical limitations associated with hardware design, signal acquisition and processing [116]. Racine [9] proposed a disturbance observer (or so-called virtual torque feedback) to estimate the interaction torque without using sensors at interaction locations, see Fig. 17 for 1-DoF joint exoskeleton.

Boaventura et al. [116] used a Kalman filter in order to estimate and filter interaction forces without using force sensors. The goal of the proposed control architecture is to make the exoskeleton imperceptible to the user by making the

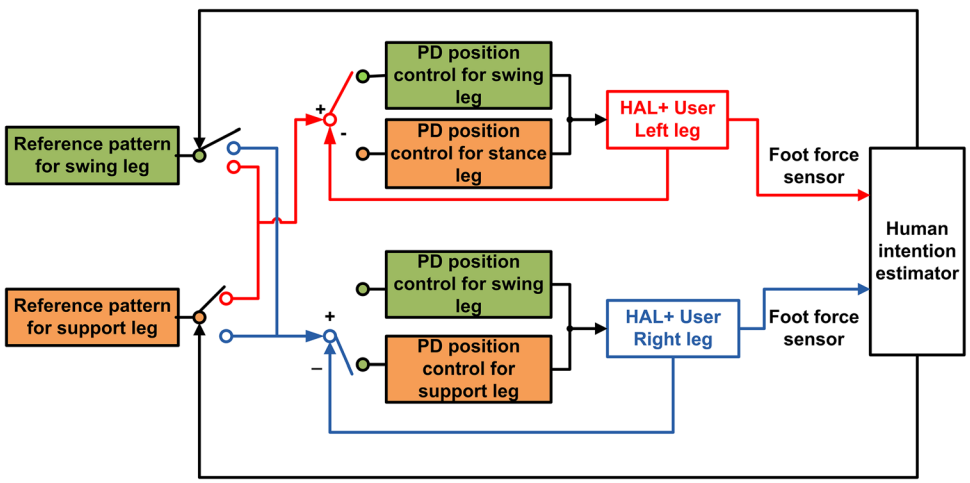

Fig. 14 The control architecture of HAL with two-level control [31–38]: the high-level control attempts to estimate the user motion intention based on force/torque sensors (p), and low-level control that includes a decoupled position control for tracking the desired references state variables for the swing and support legs

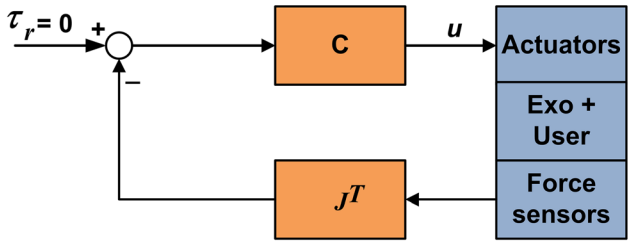

Fig. 15 Direct force control for regulation of HRI [9]

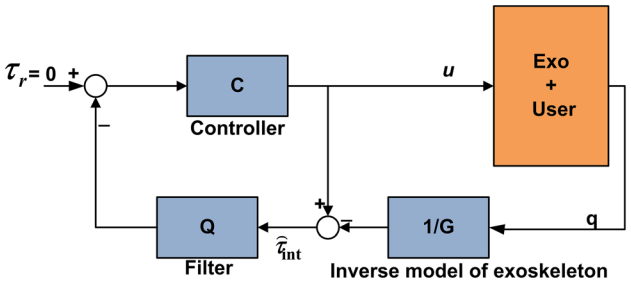

Fig. 17 Direct force control with observer base on inverse model for 1-DoF exoskeleton. $\hat{\tau}_{int}$ refers to the estimated interaction torque [9]

interaction force wrench null. The proposed control architecture includes three parallel controllers for stabilization and control of the target exoskeleton. As noted from Fig. 18, the Kalman filter design requires measurements of the exoskeleton state variables, of the desired force wrench that will be fed to the robot, and of the acceleration of the exoskeleton and of the user.

5.3.2 Control approach 2

This strategy includes the modification of exoskeleton-user trajectory in order to compensate for unwanted interaction force wrench; it is simply based on impedance/admittance principles. According to Eq. (8), the modified trajectory of exoskeleton can be written as

$$q = q_h + \frac{\tau_{int}}{k} = q_h + \delta q \tag{10}$$

Then, conventional position/velocity control can be used accordingly. HIT-LEX [42] used an inner decoupled velocity joint control associated with an outer impedance control. There are no details on the formulation of the outer impedance control; however, the schematic diagram of the proposed control refers to a mathematical relationship between the kinematic terminals (back, feet) and the sensed force/torques at these locations, see Fig. 19. This relationship can be extracted by using impedance function. In effect, the impedance control can play a significant role in transferring the multi-force sensors into displacement and vice versa.

Remark 7 As stated above, HIT-Lex [42] used F/T sensors in order to detect human motion intention; however,

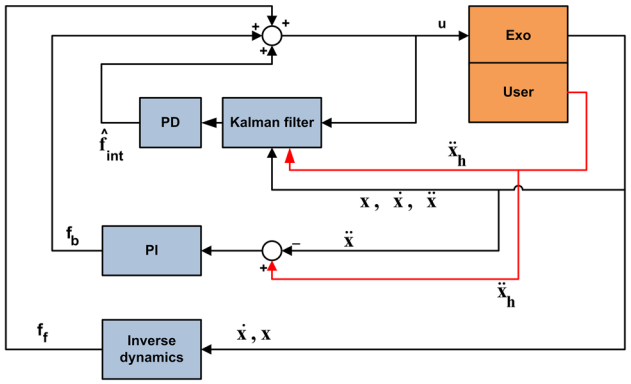

Fig. 18 Kalman filter-based transparent control for PEs [116]. The proposed controller consists of three main elements: a feedforward controller that includes inverse dynamics for generating the required force wrench, a feedback controller for precise tracking the desired user motion, and a Kalman filter for estimating the interaction force wrench and its compensation, accordingly

the designers proposed a control architecture described in Fig. 19a where the force sensors are not apparent. In view of above, the modified version of Fig. 19a is depicted in Fig. 19b that matches the experimental implementation.

Rashidi et al. [85] used a similar framework for Fig. 19 but with inner position control. The control architecture consists of an acceleration observer and of Impedance control for regulation of the human–exoskeleton interaction force wrench; the output of the impedance model is an infinitesimal change of exoskeleton positions. Lee and sankai [36] proposed active

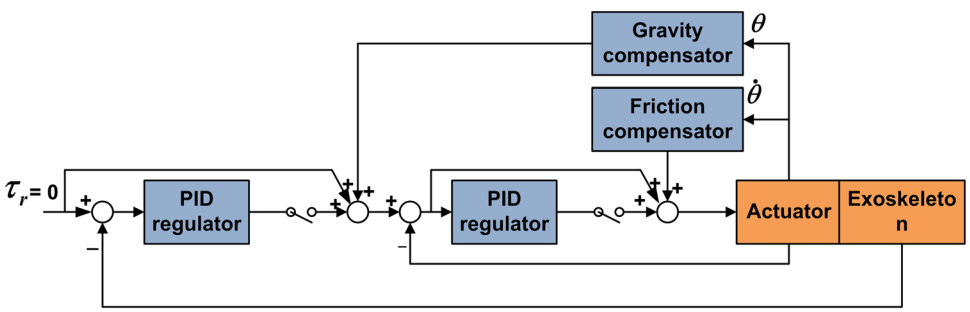

Fig. 16 Low-level control architecture with two control loops working separately for comparison purposes [115]. The control selectors are used for switching between the inner and the outer loops

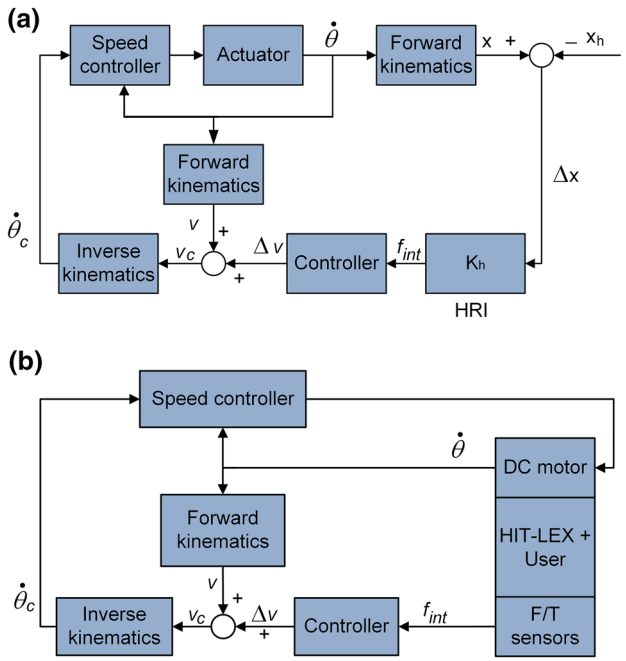

Fig. 19 Control architecture for HIT-LEX. **a** Control structure depicted in [42]; this structure is useful in simulation with nomenclature defined as follows. x refers to the end-effector position (the feet and the back), x_h denotes to the end-effector user motion, f_{int} is the interaction force wrench, v denotes to the velocity of end-effector, and θ is the angular position of joints. The authors did not describe the structure of impedance control that is necessary for regulation and stabilization of the HRI. **b** Modified version of (**a**) that matched experimental implementation

impedance control for the HAL-3 to virtually manipulate the impedance parameters of the exoskeleton with a minimized power of the user in unconstrained motion (swing phase). The proposed control strategy includes three stages: (1) identification of the user's joint dynamics parameters, (2) application of impedance control to the coupled system (exoskeleton and user) and definition of the virtual impedance parameters that minimize user power, and (3) EMG use as an assessment tool for the proposed method. A similar work can be found in [73, 117, 118]. As mentioned previously, there are some difficulties associated with interaction force wrench and human motion measurements; therefore, Kazerooni and his colleagues [6, 39–41] assumed the interaction forces are unknown in their analysis. The goal of their proposed control architecture is to amplify the user sensitivity to the interactions forces/torques without measuring them. In effect, the authors scaled down the user power by manipulating the sensitivity function that is equivalent to the admittance function. To motivate the concept of sensitivity amplification control (SAC), consider simple dynamics of a 1-DoF exoskeleton (Fig. 20).

The output angular velocity of the exoskeleton can be represented as a linear combination of the dynamic response due to the desired references (r) and the interaction torque (τ_{int}), say

$$v = Gr + S\tau_{int} \tag{11}$$

According to classical and modern control engineering [119], G and S should approach to 1 and 0 respectively, however, this could not be the case for exoskeleton design. The situation is different with exoskeleton since the required control algorithm should minimize the interaction forces/torque as possible. There is no benefit if we make S approaches zero but the interaction forces/torques are of high values! The idea is to design controller C such that d is small. To do that, let us generate a new sensitivity transfer function

$$S_d = \frac{v}{\tau_{int}} = \frac{S}{1 - GC} \tag{12}$$

In effect, S_d represents admittance dynamics with the velocity as the output and τ_{int} as the input. If we make S_d larger, this means that the target impedance is low; for larger S_d, τ_{int} should be smaller and this is the objective of exoskeleton control design. Accordingly, if a positive feedback controller is chosen as

$$C = \left(1 - \sigma^{-1}\right)G^{-1} \tag{13}$$

where σ is amplification factor greater than unity. For example if $\sigma = 10$, this results in $S_d = 10S$ which means ten times force amplification. For more details on application of the SAC for multibody exoskeletons with modified versions, see [16].

In summary, the following points are considered:

- The SAC is based on principle of admittance control and inverse dynamics principles.
- Although Yang et al. [16] proposed neural network as adaptive control with combined SAC, they did not consider different walking phases of the coupled system of the user and exoskeleton.
- More studies are required to assess performance of power assist rate generated by the SAC.

5.3.3 Control approach 3

This strategy includes adding an explicit power assist rate to the user. The assistive torques of exoskeleton are transferred to the user via interaction attachments. According to Eq. (10), if we know the required assistive torque and the impedance behaviour at the interaction locations, an explicit position control can successfully be performed as proposed in [96]. In addition, direct (explicit) force/torque control and feedforward force/torque control are two possible candidates

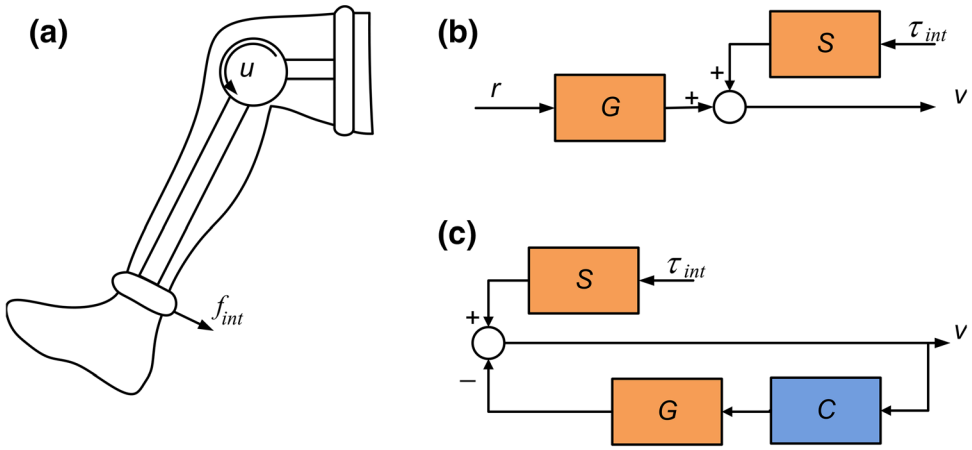

Fig. 20 Sensitive amplification control [6, 39–41]: **a** 1-DoF exoskeleton, **b** dynamics of a 1-DoF exoskeleton, and **c** the proposed feedback control

for this control point of view. Kiguchi and Hayashi [52] transferred the user muscle torques estimated through EMG to the exoskeleton actuators, using impedance model and Jacobian transformation, see Fig. 21.

Lenzi et al. [8] proposed an assistive controller consisting of three control stages: estimating of walking phase (online), planning of the assistive torque, and providing the power assist rate to the hip joint only, recall Fig. 11 for more details. According to Fig. 11, the high-level control attempts to calculate desired hip torque considering the power assist rate as a set point to the low-level control, whereas low-level control attempts to track the desired reference torque by feeding back the interaction torque measured by force/torque sensors at the cuff. Thanks to measured interaction torque, the feedback torque can mask the robotic leg inertia with feedforward gravity and friction compensation. The work of Kazerroni and his colleagues [6, 39–41], mentioned previously, can determine the required assistive power rate by using sensitivity function.

Remark 8 Based on the previous control approaches, the low-level control architecture can be sub-divided into three categories: indirect force control, direct force control, and observer-base control. Please, see the remarks below and Table 2 that summarizes features and limitations of the aforementioned control strategies.

Remark 9 The following points can be noted concerning indirect force control:

- The key point of impedance control is to generate a virtual impedance model of exoskeleton that matches the variable behavior impedance of the user at interaction locations, considering minimization of user's stress. This point is considered a little with a single joint exoskeleton as proposed in [36, 73].
- Some studies focus on precisely tracking the exoskeleton and making interaction force wrench null without considering explicitly the power assist rate required by the user.
- There are two possible techniques for capturing the required power assist rate data from the user: EMG technique and time-varying parameters impedance control.

Remark 10 The following points are considered for direct force control:

- Direct force control includes tracking desired interaction torque control considering power assist rate. As a result, high-level control is required in order to estimate the reference torque carefully as proposed in [8].
- Torque feedback control requires F/T sensors at interaction attachments of exoskeleton and the user. A force/torque observer can be used for evading sensor measurements in practice.

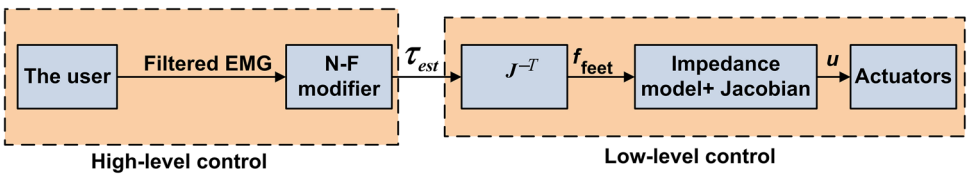

Fig. 21 EMG-based control with multi-stages control [52], where τ_{est} is the estimated joint torques for the user, f is the foot force vector for the user, J is the Jacobian, and u is the input control considering the power assist rate. There is a hidden level of control associated with user's balance control; it is eliminated here since this paper is concerned with non-disabled users

Table 2 Features and Limitations of Low-level Control Strategies

Control strategy	Description
Position control/indirect force control/control approach 1	It is a model-free controller that does not need full knowledge of the LEE dynamics Measurement of the user motion is required The gravity, the friction degree, and different motion constraints should be integrated with the control architecture
Impedance/admittance control/indirect force control/control approach 2	It is a powerful tool for stabilization control of constrained system such as the LEE The variable impedance parameters should carefully be considered otherwise instability issues can occur The power assist rate can explicitly/implicitly be integrated
F/T feedback control (direct F/T control) (This strategy can be designed based on control approach 1,3 and even 2 if force tracking-based admittance control is proposed)	It requires F/T sensors The power assist rate can explicitly be integrated High-level control is necessary for estimation of the desired joint torques
Feedforward torque control (direct F/T control) Control approach 3	It requires EMG for estimation of the joint torques The EMG can have some practical limitations The power assist rate can explicitly be integrated
Observer-based force control (most control approaches can be modified to make force observer)	It does not require F/T sensors It may require the measurements of state variables for the user that could not be straightforward

- Admittance control can be used with two control loops: an outer admittance control for torque tracking and an inner position/velocity control for position/velocity tracking.

Remark 11 In summary, the following points are considered for force observer-based control:

- There is little work on observer-based force control for the LEEs. However, Fig. 18 proposed a Kalman filter for interaction force wrench but with measurements of acceleration, velocity and position.
- Kazerooni and his team [6, 39–41] proposed sensitivity amplification control (SAC) without requirement of interaction force wrench and applied it to Bleex. Limitations of their technique is its sensitivity to the uncertainty of the host system. An improved version is proposed by [16].
- The power assist rate is not integrated in Fig. 18, whereas amplification factor is considered carefully in the SAC.

Remark 12 The essential difference between non-disabled and disabled users lies in the capabilities of the formers to compensate for any possible disturbance and deviated references by using their own control systems. Therefore, some balance criteria are used in literature for disabled users as proposed in [18–20]. However, balance control strategy combined with ZMP was also user for non-disabled users with wearable exoskeletons as made in [120].

Remark 13 In summary, Table 3 described some well-known LEEs with power augmentation.

6 Conclusions

This paper attempts to summarize and overview major issues associated with movement and control of LEEs destined to be used by non-disabled people, for force augmentation. There are four major points should be considered while designing the control architecture for the host exoskeleton: (1) estimation of user motion intention, (2) minimization of human–machine interaction, (3) estimation of interaction force wrench for control purpose; an observer is preferred in order to evade practical limitations, and (4) determination of power assist rate required for force augmentation. Most researchers concentrate on some important points and neglect others, as stated throughout the paper. It should be noted that determination of the power assist rate requires knowledge of the user joint torques during walking (EMG used for this purpose). In addition, using EMG-based control gives higher mechanical advantage than force control strategies, but at the expense of associated computational complexity and EMG issues. More studies are required to assess the difficulties and the computational complexities of the present control strategies.

Table 3 Some state of art LEEs for power augmentation[a,b]

Name	Year and country	Purpose	Actuator type	Dynamics	Active/Passive DOF	High-level control	Mid-level control	Low-level control
Wearable Power Assisting Suit [122, 123]	Since 1991-Japan	It is designed to give the nurse additional power for helping the patients.	Pneumatic actuators	Lagrange formulation-based multibody dynamics	6 active DOFs at the elbows, waist and knees	Muscle hardness sensors (bioelectrical sensors)	N/A[c]	Feedforward torque control[d]
HAL-5 [31–38]	Since 1992-Japan	It is an updated version of the HAL systems dedicated to augment and support the human capabilities. Although it is particularly designed for people with physical disabilities, it is able to enhance the user power and help the non-disable people to carry heavy loads.	Electrical DC motors	Multibody dynamics are not required and only actuator dynamics are required	8 active DOFs in total: 1 DOF-shoulder joint 1 DOF-elbow joint 1 DOF-hip joint 1 DOF-knee joint	EMG-based technique + F/T sensors	GRFs	Pure position control
RoboKnee [7]	Since 2001-USA	It is designed to enhance the capability of the legs while carrying a heavy load in the backpack.	Electrical DC SEAs	Only the knee actuator dynamics are required	1 active DOF at the knee	F/T sensors + knee angle	GRFs	Force control
BLEEX [6, 39–41]	Since 2004-USA	It consists of two anthropomorphic legs, power units, and backpack-like frame for carrying loads.	Hydraulic actuators	Lagrange formulation-based multibody dynamics	16 active/passive DOFs in total:[e] 3 DOFs-hip joint 1 DOF-knee joint 3 DOFs-ankle joint 1 passive DOF-foot	Not required	GRFs	The SAC strategy
Quasi-passive MIT Exoskeleton [2–5]	Since 2006-USA	It is designed to perform improved metabolic performance as compared to the standard actuated exoskeletons.	Electrical DC SEAs	Only the actuator dynamics are required	6 active/passive DOFs in total: 1 active DOF at the hip joint 1 Variable damper at the knee joint 1 Passive spring at the ankle joint.	Shank strain gauges + Actuator potentiometers	GRFs + joint angles/velocities with state machine control	Force control for the hip joints

Table 3 (continued)

Name	Year and country	Purpose	Actuator type	Dynamics	Active/Passive DOF	High-level control	Mid-level control	Low-level control
The Body Extender BE [87, 124]	Since 2011-Italy	It is designed to assist human for carrying load considering irregular terrains.	Electrical DC motors	–	22 active DOFs in total: 2 DOFs-ankle joint 1 DOF-knee joint 3 DOFs-hip joint 2 DOFs-shoulder joint 1 DOF-elbow joint 2 DOFs-wrist joint 1 DOF-hand	F/T sensors	GRFs with state machine control	Admittance control with an inner velocity control loop
HIT-LEX [42]	Since 2016-China	–	–	–	14 active/passive DoFs in total:[f] 3 DoF-hip joint, 1 DoF-knee, 2 DoF–ankle joint, and 2 DoF–waist	–	–	–

[a]There are other LEEs manufactured for enhancing the human capabilities and transferring heavy loads but no detailed information is available; see e.g., [125–127]

[b]This table is focused on LEEs with carrying-load activities; the reader is referred to [43–49] for more details on rehabilitation wearable robots

[c]The experiments were focused on lifting/lower a specific weight and hence no a mid-level control algorithm was required

[d]The input control torque of the LEE consists of the user muscle sensors-based joint torques and the dynamic model-based torques required to maintain a position of a lifting a patient

[e]The joints are actuated in the sagittal plane only

[f]Only four joints are actuated for the sagittal movements (hip and knee joints only), whereas the others are passively balanced by springs

Acknowledgements This work was supported by the Postdoctoral Fellowship of Shandong University, School of Control Science and Engineering, China, and the COST Action CA 16116—Wearable Robots for Augmentation, Assistance or Substitution of Human Motor Functions.

Compliance with ethical standards

Conflict of interest The authors declare that they have no conflict of interest.

References

1. Li Z, Xie H, Li W, Yao Z (2014) Proceeding of human exoskeleton technology and discussions on future research. Chin J Mech Eng 27:437–447. https://doi.org/10.3901/CJME.2014.03.437
2. Walsh J (2006) Biomimetic design of an under-actuated leg exoskeleton for load-carrying augmentation. M.S. Thesis, Massachusetts Institute of Technology
3. Walsh J, Pasch K, Herr H (2006) An autonomous, underactuated exoskeleton for load-carrying augmentation. In: IEEE/RSJ international conference on intelligent robots and systems, pp 1410–1415
4. Walsh J, Paluska D, Pasch K, Grand W, Valiente A, Herr H (2006) Development of a lightweight, underactuated exoskeleton for load-carrying augmentation. In: IEEE international conference on robotics and automation (ICRA), Florida, USA, pp 3485–3491
5. Walsh J, Endo K, Herr H (2007) A quasi-passive leg exoskeleton for load-carrying augmentation. Int J Hum Robot 04:487–506
6. Kazerooni H, Steger R (2005) The Bekeley lower extremity exoskeleton. J Dyn Syst Meas Control 128:14–25
7. Pratt E, Krupp T, Morse J, Collins H (2004) The RoboKnee: an exoskeleton for enhancing strength and durance during walking. In: 2004 IEEE international conference on robotics and automation, ICRA'04, vol 3, pp 2430–2435
8. Lenzi T, Carrozza MC, Agrawal SK (2013) Powered hip exoskeletons can reduce the user's hip and ankle muscle activations during walking. IEEE Trans Neural Syst Rehabil Eng 21:938–948
9. Racine J-LC (2003) Control of a lower extremity exoskeleton for human performance amplification. PhD Dissertation, University of California, Berkeley
10. Yagin N (1890) Apparatus for facilitating walking. U.S. Patent
11. Kelley CL (1919) Pedomotor. U.S. Patent
12. Mizen NJ (1978) Preliminary design of a full-scale, wearable, exoskeletal structure. Final report, Cornell Aeronautical Laboratory, inc
13. Mizen, NJ (1964) Design and test of a full-scale, wearable, exoskeletal structure. Interim Technical Report
14. Mosher RS (1960) Force-reflecting electrohydraulic manipulator. Electro-Technology
15. Makinson JB (1971) Research and development prototype for machine augmentation of human strength and endurance: Hardiman I project. General Electric Report S-71-1056, Schenectady, NY
16. Yang Z, Gu W, Zhang J, Gui L (2017) Force control theory and method of human load carrying exoskeleton suit. Springer, National Defense Industry Press, Berlin
17. Rosheim M (1994) Robot evolution: the development of anthrobotics, 1st edn. Wiley-Interscience, New York
18. Hristic D, Vukobratovic M (1973) Development of active aids for handicapped. In: Proceedings of the III international conference on bio-medical engineering, Sorrento, Italy
19. Vukobratovic M, Ciric V, Hristic D (1972) Contribution to the study of active exoskeletons. In: Proceedings of the 5th IFAC congress, Paris, vol 5, pp 88–96
20. Vukobratovic M (2007) When were active exoskeletons actually born. Int J Hum Robot 04:459
21. Al-Shuka HFN, Corves B, Zhu W-H, Vanderborght B (2016) Multi-level control of zero-moment point-based humanoid biped robots: a review. Robotica 34:2440–2466
22. Al-Shuka HFN (2014) Modeling, walking pattern generators and adaptive control of biped robot. PhD Dissertation, RWTH Aachen University, Germany
23. Al-Shuka HFN, Allmendinger F, Corves B, Zhu W-H (2014) Modeling, stability and walking pattern generators of biped robots: a review. Robotica 32:907–934
24. Al-Shuka HFN, Corves B, Vanderborght B, Zhu W-H (2015) Zero-moment point-based biped robot with different walking patterns. Int J Intell Syst Appl 01:31–41
25. Al-Shuka HFN, Corves B (2013) On the walking pattern generators of biped robot. J Autom Control Eng 1:149–155
26. Al-Shuka HFN, Corves B, Zhu W-H, Vanderborght B (2014) A simple algorithm for generating stable biped walking patterns. Int J Comput Appl 101:29–33
27. Al-Shuka HFN, Corves B, Zhu W-H (2014) Function approximation technique-based adaptive virtual decomposition control for a serial-chain manipulator. Robotica 32:375–399
28. Al-Shuka HFN (2018) On local approximation-based adaptive control with applications to robotic manipulators and biped robots. Int J Dyn Control 6:339–353. https://doi.org/10.1007/s40435-016-0302-6
29. Al-Shuka HFN, Corves B, Zhu W-H (2014) Dynamic modeling dynamic modeling of biped robot using lagrangian and recursive newton-euler formulations. Int J Comput Appl 101:1–8
30. Al-Shuka HFN, Corves B, Zhu W-H (2013) On the dynamic optimization of biped robot. Lect Notes Softw Eng 1:237–243
31. Sankai Y (2010) HAL: hybrid assistive limb based on cybernics. In: Proceedings of the robotics research 13th international symposium, pp 25–34
32. Suzuki K, Kawamura Y, Hayashi T, Sakurai T, Hasegawa Y, Sankai Y (2005) Intention-based walking support for paraplegia patient. IEEE Int Conf Syst Man Cybernet 3:2707–2713
33. Toda H, Kobayakawa T, Sankai Y (2006) A multi-link system control strategy based biologilcal movement. Adv Robot 20:661–679
34. Toda H, Sankai Y (2006) Three-dimensional link dynamics simulator base on n-single-particle movement. Adv Robot 19:977–993
35. Kawamoto H, Sankai Y (2005) Power assist method based on phase sequence and muscle force condition for HAL. Adv Robot 19:717–734
36. Lee S, Sankai Y (2005) Virtual impedance adjustment in unconstrained motion for exoskeletal robot assisting lower limb. Adv Robot 19:773–795
37. Suzuki K, Mito G, Kawamoto H, Hasegawa Y, Sankai Y (2007) Intention-based walking support for paraplegia patients with robot suit hal. Adv Robot 21:1441–1469
38. Kawamoto CH, Sankai Y (2002) Comfortable power assist control method for walking aid by hal-3. In: IEEE international conference on systems, man and cybernetics, vol 4
39. Chu A, Kazerooni H, Zoss A (2005) On the biomimetic design of the Berkeley lower extremity exoskeleton (bleex). In: IEEE international conference on robotics and automation, April, Barcelona, pp 4345–4352
40. Kazerooni H, Racine, JL, Huang L, Steger R (2005) On the control of the Berkeley lower extremity exoskeleton (bleex). In: IEEE international conference on robotics and automation, Barcelona, pp 4353–4360

41. Zoss A, Kazerooni H (2005) On the mechanical design of the Berkeley lower extremity exoskeleton. In: IEEE intelligent robots and systems conference, pp 3465–3472
42. Zhang C, Zang X, Leng Z, Yu H, Zhao J, Zhu Y (2016) Human–machine force interaction design and control for the HIT load-carrying exoskeleton. Adv Mech Eng 8:1–14
43. Jiménez-Fabián R, Verlinden O (2011) Review of control algorithms for robotic ankle systems in lower-limb orthoses, prostheses, and exoskeletons. Med Eng Phys 34:397–408
44. Díaz I, Gil JJ, Sánchez E (2011) Lower-limb robotic rehabilitation: literature review and challenges. J Robot 2011:759764. https://doi.org/10.1155/2011/759764
45. Anam K, Al-Jumaily A (2012) Active exoskeleton control systems: state of the art. International Symposium on Robotics and Intelligent Sensors 2012 (IRIS 2012). Procedia Eng 41:988–994
46. Yan T, Cempini M, Oddo CM, Vitiello N (2015) Review of assistive strategies in powered lower-limb orthoses and exoskeletons. Robot Auton Syst 64:120–136. https://doi.org/10.1016/j.robot.2014.09.032
47. Chen B et al (2016) Recent developments and challenges of lower extremity exoskeletons. J Orthop Transl 5:26–37
48. Li N et al (2015) Review on lower extremity exoskeleton robot. Open Autom Control Syst J 7:441–453
49. Rupal B et al (2017) Lower-limb exoskeletons: research trends and regulatory guidelines in medical and non-medical applications. Int J Adv Robot Syst. https://doi.org/10.1177/1729881417743554
50. Whittle M (2006) An introduction to gait cycle, 4th edn. Butterworth-Heinemann, Edinburgh
51. Neumann DA (2009) Kinesiology of the musculoskeletal system: foundations for physical rehabilitation, 2nd edn. Mosby, New York
52. Kiguchi K, Imada Y (2009) EMG-based control of a lower-limb power-assist robot. In: 2009 IEEE workshop on robotic intelligence in informationally structured space, pp 19–24
53. Martinez-Villalpando EC, Herr H (2009) Agonist-antagonist active knee prosthesis: a preliminary study in level-ground walking. J Rehabil Res Dev 46:361–373
54. Shamaei K, Cenciarini M, Dollar AM (2001) On the mechanics of the ankle in the stance phase of the gait. In: 33rd annual international conference of the IEEE EMBS Boston, Massachusetts USA, pp 8135–8140
55. Kim H-G, Lee J-W, Jang J, Park S, Han C (2015) Design of an exoskeleton with minimized energy consumption based on using elastic and dissipative elements. Int J Control Autom Syst 13:463–474
56. Attwells RL, Birrell SA, Hooper RH, Mansfield NJ (2006) Influence of carrying heavy loads on soldiers' posture, movements and gait. Ergonomics 49:1527–1537
57. Bobet J, Norman RW (1984) Effects of load placement on back muscle activity in load carriage. Eur J Appl Physiol 53:71–75
58. Schulze C, Lindner T, Schulz K, Woitge S, Mittelmeier W, Bader R (2012) Influence of increased load wearing on human posture and muscle activation of trunk and lower limb. Swiss Med Wkly 142:4–5
59. Knapik J, Harman E, Reynolds K (1996) Load carriage using packs: a review of physiological, biomechanical and medical aspects. Appl Ergon 27:207–216
60. Lindner T, Schulze C, Woitge S, Finze S, Mittelmeier W, Bader R (2012) The effect of the weight of equipment on muscle activity of the lower extremity in soldiers. Sci World J 2012:976513. https://doi.org/10.1100/2012/976513
61. Vanderborght B et al (2013) Variable impedance actuators: a review. Robot Autonom Syst 61:1601–1614
62. Li Z, Huang Z, He W, Su CY (2017) Adaptive impedance control for an upper limb robotic exoskeleton using biological signals. IEEE Trans Ind Electron 64:1664–1674
63. Lawrence DA (1988) Impedance control stability properties in common implementations. In: IEEE international conference on robotics and automation, vol 2, pp 1185–1190
64. Ali M (2011) Impedance control of redundant manipulators. PhD Dissertation, Tampere University of Technology, Finland
65. Ott C (2008) Cartesian impedance control of redundant and flexible-joint robots. Springer Tracts in Advanced Robotics
66. Dietrich A (2016) Whole-body impedance control of wheeled humanoid robots. Springer Tracts in Advanced Robotics
67. Huang A-C, Chien M-C (2010) Adaptive control of robot manipulators: a unified regressor-free approach. World Scientific, Singapore
68. Al-Shuka H, Leonhardt S, Zhu W-H, Song R, Ding C, Li Y (2018) Active impedance control of bioinspired motion robotic manipulators: an overview. Appl Bion Biomech 2018:8203054. https://doi.org/10.1155/2018/8203054
69. Głowiński S, Krzyżyński T (2016) An inverse kinematic algorithm for the human leg. J Theor Appl Mech 54:53–61. https://doi.org/10.15632/jtam-pl.54.1.53
70. Zakaria MA, Abdul Majeed APP, Khairuddin IM, Taha Z (2017) Kinematics analysis of a 3dof lower limb exoskeleton for gait rehabilitation: a preliminary investigation. In: Ibrahim F, Cheong J, Usman J, Ahmad M, Razman R, Selvanayagam V (eds) 3rd international conference on movement, health and exercise. MoHE 2016. IFMBE proceedings, vol 58. Springer, Singapore
71. Zhu W-H (2010) Virtual decomposition control: toward hyper degrees of freedom robots. Springer, Berlin
72. Luna CO, Rahman MH, Saad M, Archambault PS, Zhu W-H (2016) Virtual decomposition control of an exoskeleton robot arm. Robotica 34:1587–1609
73. Aguirre-Ollinger G, Colgate JE, Peshkin MA, Goswami A (2007) Active-impedance control of a lower-limb assistive exoskeleton. In: 10th IEEE international conference on rehabilitation robotics, pp 188–195
74. Huo W, Huo Mohammed S, Amirat Y (2015) Observer-based active impedance control of a knee-joint assistive orthosis. In: IEEE international conference on rehabilitation robotics (ICORR), pp 313–318
75. Gregg RD, Lenzi T, Hargrove LJ, Sensinger JW (2014) Virtual constraint control of a powered prosthetic leg: from simulation to experiments with transfemoral amputees. IEEE Trans Robot 30:1455–1471
76. Lv G, Zhu H, Elery T, Li L, Gregg RD (2016) Experimental implementation of underactuated potential energy shaping on a powered ankle-foot orthosis. In: IEEE international conference on robotics and automation, pp 3493–3500
77. Westervelt ER, Grizzle JW, Chevallereau C, Choi JH, Morris B (2007) Feedback control of dynamic bipedal robot locomotion. CRC, New York
78. Sreenath K, Park H-W, Poulakakis I, Grizzle JW (2011) A compliant hybrid zero dynamics controller for stable, efficient and fast bipedal walking on MABEL. Int J Robot Res 30:1170–1193
79. Kolathaya S, Ames AD (2012) Achieving bipedal locomotion on rough terrain through human-inspired control. In: IEEE international symposium on safety security rescue robot, College Station, TX, USA, pp 1–6
80. Martin A, Post D, Schmiedeler J (2014) Design and experimental implementation of a hybrid zero dynamics controller for planar bipeds with curved feet. Int J Robot Res 33:988–1005
81. Ramezani A, Hurst JW, Hamed KA, Grizzle JW (2013) Performance analysis and feedback control of ATRIAS, a 3D bipedal robot. ASME J Dyn Syst Meas Control 136:021012

82. Boaventura T, Buchli J, Semini C, Caldwell D (2015) Model-based hydraulic impedance control for dynamic robots. IEEE Trans Robot 31:1324–1336
83. Best CM (2016) Position and stiffness control of inflatable robotic links using rotary pneumatic actuation. MSc Dissertation, Brigham Young University, USA
84. Vallery H et al (2008) Compliant actuation of rehabilitation robots: benefits and limitations of series elastic actuators. IEEE Robot Autom Mag 15:60–69
85. Rashidi A, Zibafar A, Khezrian R, Vossoughi G (2015) Design and performance analysis of a transparent force control strategy for an exoskeleton. In: 3rd RSI international conference on robotics and mechatronics (ICROM), pp 563–568
86. Deng X, Shen H, Chen F, Yu Y, Ge Y (2007) Motion information acquisition from human lower limbs for wearable robot. In: International conference on information acquisition, pp 137–142
87. Fontana M et al (2014) The body extender: a full-body exoskeleton for the transport and handling of heavy loads. IEEE Robot Autom Mag 21:34–44
88. Simone M, Fabio S, Marco F, Massimo B (2011) Body extender: whole body exoskeleton for human power augmentation. In: IEEE international conference on robotics and automation, Shanghai, China, pp 611–616
89. Chu G, Hong J, Jeong D-H, Kim D, Kim S, Jeong S, Choo J (2014) The experiments of wearable robot for carrying heavy-weight objects of shipbuilding works. In: 2014 IEEE international conference on automation science and engineering (CASE), Taipei, Taiwan, pp 978–983
90. The Active Link Co. Ltd. http://activelink.co.jp/15. Accessed 1 Sept 2018
91. Tomoyuki I, Tsuyoshi K, Koichi O, Go S, Reishi O, Hiromichi F (2010) Movement analysis of power-assistive machinery with high strength-amplification. In: Proceeding of SICE annual conference, Taipei, Taiwan, pp 2022–2025
92. Rahman MH, Ouimet TK, Saad M, Kenne JP, Archambault PS (2012) Development of a 4 DoFs exoskeleton robot for passive arm movement assistance. Int J Mechatron Autom 2:34–50
93. Rahman MH, Luna CO, Saad M, Archambault P (2015) EMG based control of a robotic exoskeleton for shoulder and elbow motion assist. J Autom Control Eng 3:270–276
94. Winter DA (2009) Biomechanics and motor control of human movement. 4th Edition, John Wiley & Sons, Inc
95. Sekine M, Gonzalez J, Tames JG, Yu W (2013) Variable impedance control based on impedance estimation model with EMG signals during extension and flexion tasks for a lower limb rehabilitation robotic system. J Nov Physiother 3:178. https://doi.org/10.4172/2165-7025.1000178
96. Kim S, Bae J (2014) Development of a lower extremity exoskeleton system for human–robot interaction. In: The 11th international conference on ubiquitous robots and ambient intelligence, pp 132–135
97. Multon F (2013) Sensing human walking: algorithms and techniques for extracting and modeling locomotion. In: Steinicke F, Visell Y, Campos J, Lécuyer A (eds) Human walking in virtual environments. Springer, New York
98. Olivier AH, Crétual A (2007) Velocity/curvature relations along a single turn in human locomotion. Neurosci Lett 412:148–153
99. Pozzo T, Berthoz A, Lefort L, Vitte E (1991) Head stabilization during various tasks in humans. II. Patients with bilateral vestibular deficits. Exp Brain Res 85:208–217
100. Kavanagh J, Barett R, Morrison R (2005) Age-related differences in head and trunk coordination during walking. Hum Mov Sci 24:574–587
101. Zhang B, Jiang S, Wei D, Marschollek M, Zhang W (2012) State of the art in gait analysis using wearable sensors for healthcare applications. In: IEEE/ACIS 11th international conference on computer and information science, pp 213–218
102. Chen X (2013) Human motion analysis with wearable inertial sensors. PhD Dissertation, University of Tennessee, USA
103. Chinmilli P, Redkar S, Zhang W, Sugar T (2017) A Review on wearable inertial tracking based human gait analysis and control strategies of lower-limb exoskeletons. Int Robit Autom J 3:00080. https://doi.org/10.15406/iratj.2017.03.00080
104. Glowinski S, Blazejewski A, Krzyzynski T (2017) Human gait feature detection using inertial sensors wavelets. In: González-Vargas J, Ibáñez J, Contreras-Vidal J, van der Kooij H, Pons J (eds) Wearable robotics: challenges and trends. Biosystems & biorobotics, vol 16. Springer, Cham
105. Sprager S, Juric MB (2015) Inertial sensor-based gait recognition: a review. Sensors 15:22089–22127
106. Byun S et al (2018) Gait variability can predict the risk of cognitive decline in cognitively normal older people. Dement Geriatr Cogn Disord 45(5–6):251–261. https://doi.org/10.1159/000489927
107. Seel T, Schauer T, Raisch J (2014) IMU-based joint angle measurement for gait analysis. Sensors 14:6891–6909. https://doi.org/10.3390/s140406891
108. Ben Mansour K, Rezzoug N, Gorce P (2015) Analysis of several methods and inertial sensors locations to assess gait parameters in able-bodied subjects. Gait Posture 42:409–414. https://doi.org/10.1016/j.gaitpost.2015.05.020
109. Caldas R et al (2017) A systematic review of gait analysis methods based on inertial sensors and adaptive algorithms. Gait Posture 57:204–210. https://doi.org/10.1016/j.gaitpost.2017.06.019
110. Totaro M et al (2017) Soft smart garments for lower limb joint position analysis. Sensors (Basel) 17(10):2314. https://doi.org/10.3390/s17102314
111. Cifuentes CA, Frizera A (2016) Human–robot interaction strategies for walker-assisted locomotion. Springer, Berlin
112. Taborri J, Palermo E, Rossi S, Cappa P (2016) Gait partitioning methods: a systematic review. Sensors 16:66. https://doi.org/10.3390/s16010066
113. Siciliano B, Villani L (1999) Robot force control. The Springer International Series in Engineering and Computer Science
114. Duong MK, Cheng H, Toan HT, Jing Q (2016) Minimizing human–exoskeleton interaction force using compensation for dynamic uncertainty error with adaptive rbf network. J Intell Robot Syst 82:413–433
115. Zanotto D, Lenzi T, Stegall P, Agrawal SK (2013) Improving transparency of powered exoskeletons using force/torque sensors on the supporting cuffs. In: IEEE 13th international conference on rehabilitation robotics (ICORR), pp 1–6
116. Boaventura T, Hammer L, Buchli J (2016) Interaction force estimation for transparency control on wearable robots using a Kalman filter. Converging clinical and engineering research on neurorehabilitation II, pp 489–493
117. Tsuji T, Tanaka Y, Kaneko M (2001) Tracking control properties of human–robot systems. In: Proceedings of the 1st international conference on information technology in mechatronics, Istanbul, pp 77–83
118. Yamada Y, Konosu H, Morizono T, Umetani Y (1999) Proposal of skill-assist: a system of assisting human workers by reflecting their skills in positioning tasks. In: Proceedings of the IEEE international conference on systems, man and cybernetics, Tokyo, pp (IV)11–(IV)16
119. Wilkie J, Johnson MA, Katebi R (2001) Control engineering: an introductory course. Palgrave
120. Liu X, Low KH, Yu HY (2004) Development of a lower extremity exoskeleton for human performance enhancement. In:

Proceedings 01 2004 IEEE/RSJ international conference on intelligent robots and systems, pp 3889–3894
121. Rechy-Ramirez EJ, Hu H (2011) Stages for developing control systems using EMG and EEG signals: a survey. Technical report: CES-513, University of Essex, ISSN 1744-8050
122. Yamamoto K, Ishii M, Hyodo K, Yoshimitsu T, Matsuo T (2003) Development of power assisting suit (miniaturization of supply system to realize wearable suit). JSME Int J Ser C 46:923–930
123. Yamamoto K, Ishii M, Noborisaka H, Hyodo K (2004) Stand alone wearable power assisting suit-sensing and control systems. In: 3th IEEE international workshop on robot and human interactive communication (IEEE Catalog No. 04TH8759), pp 661–666
124. Lucchesi N et al (2010) An approach to the design of fully actuated body extenders for material handling. In: 19th international symposium in robot and human interactive communication, pp 482–487
125. Kazerooni H, Harding N, Angold R (2006) Lower extremity exoskeleton. International Patent, WO2006/078871A2
126. Kazerooni H, Harding N, Angold R, Amundson K, Burns JW, Zoss A (2010) Wearable material handling system. International Patent, WO2010/101595A1
127. Sarcos R(2010) Control logic for biomimetic joint actuators. International Patent, WO2010/025403A1

Terms and Conditions

Springer Nature journal content, brought to you courtesy of Springer Nature Customer Service Center GmbH (“Springer Nature”).
Springer Nature supports a reasonable amount of sharing of research papers by authors, subscribers and authorised users (“Users”), for small-scale personal, non-commercial use provided that all copyright, trade and service marks and other proprietary notices are maintained. By accessing, sharing, receiving or otherwise using the Springer Nature journal content you agree to these terms of use (“Terms”). For these purposes, Springer Nature considers academic use (by researchers and students) to be non-commercial.
These Terms are supplementary and will apply in addition to any applicable website terms and conditions, a relevant site licence or a personal subscription. These Terms will prevail over any conflict or ambiguity with regards to the relevant terms, a site licence or a personal subscription (to the extent of the conflict or ambiguity only). For Creative Commons-licensed articles, the terms of the Creative Commons license used will apply.
We collect and use personal data to provide access to the Springer Nature journal content. We may also use these personal data internally within ResearchGate and Springer Nature and as agreed share it, in an anonymised way, for purposes of tracking, analysis and reporting. We will not otherwise disclose your personal data outside the ResearchGate or the Springer Nature group of companies unless we have your permission as detailed in the Privacy Policy.
While Users may use the Springer Nature journal content for small scale, personal non-commercial use, it is important to note that Users may not:

1. use such content for the purpose of providing other users with access on a regular or large scale basis or as a means to circumvent access control;
2. use such content where to do so would be considered a criminal or statutory offence in any jurisdiction, or gives rise to civil liability, or is otherwise unlawful;
3. falsely or misleadingly imply or suggest endorsement, approval , sponsorship, or association unless explicitly agreed to by Springer Nature in writing;
4. use bots or other automated methods to access the content or redirect messages
5. override any security feature or exclusionary protocol; or
6. share the content in order to create substitute for Springer Nature products or services or a systematic database of Springer Nature journal content.

In line with the restriction against commercial use, Springer Nature does not permit the creation of a product or service that creates revenue, royalties, rent or income from our content or its inclusion as part of a paid for service or for other commercial gain. Springer Nature journal content cannot be used for inter-library loans and librarians may not upload Springer Nature journal content on a large scale into their, or any other, institutional repository.
These terms of use are reviewed regularly and may be amended at any time. Springer Nature is not obligated to publish any information or content on this website and may remove it or features or functionality at our sole discretion, at any time with or without notice. Springer Nature may revoke this licence to you at any time and remove access to any copies of the Springer Nature journal content which have been saved.
To the fullest extent permitted by law, Springer Nature makes no warranties, representations or guarantees to Users, either express or implied with respect to the Springer nature journal content and all parties disclaim and waive any implied warranties or warranties imposed by law, including merchantability or fitness for any particular purpose.
Please note that these rights do not automatically extend to content, data or other material published by Springer Nature that may be licensed from third parties.
If you would like to use or distribute our Springer Nature journal content to a wider audience or on a regular basis or in any other manner not expressly permitted by these Terms, please contact Springer Nature at

onlineservice@springernature.com